AD-A163 974 EFFECTS OF SURFACE ROUGHNESS ON PRESSURE DISTRIBUTION AND BOUNDARY LAYER..(U) AIR FORCE INST OF TECH WRIGHT-PATTERSON AFB OH SCHOOL OF ENGI.. L D WILLIAMS 1/1

UNCLASSIFIED DEC 85 AFIT/GAE/AA/85D-17 F/G 20/4 NL

END

FILMED

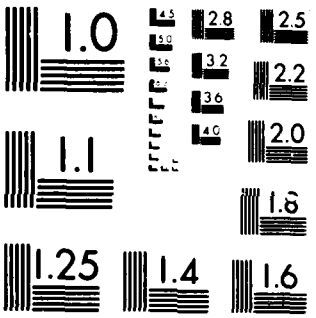

EFFECTS OF SURFACE ROUGHNESS ON PRESSURE DISTRIBUTION AND BOUNDARY LAYER OVER COMPRESSOR BLADES AT HIGH REYNOLDS NUMBER IN A TWO-DIMENSIONAL CASCADE

THESIS

Larry D. Williams, B.S.
Captain, USAF

AFIT/GAE/AA/85D-17

DEPARTMENT OF THE AIR FORCE
AIR UNIVERSITY
AIR FORCE INSTITUTE OF TECHNOLOGY

Wright-Patterson Air Force Base, Ohio

AFIT/GAE/AA/85D-17

EFFECTS OF SURFACE ROUGHNESS ON PRESSURE DISTRIBUTION AND BOUNDARY LAYER OVER COMPRESSOR BLADES AT HIGH REYNOLDS NUMBER IN A TWO-DIMENSIONAL CASCADE

THESIS

Larry D. Williams, B.S.
Captain, USAF

AFIT/GAE/AA/85D-17

AFIT/GAE/AA/85D-17

EFFECTS OF SURFACE ROUGHNESS ON PRESSURE DISTRIBUTION AND BOUNDARY LAYER OVER COMPRESSOR BLADES AT HIGH REYNOLDS NUMBER IN A TWO-DIMENSIONAL CASCADE

THESIS

Presented to the Faculty of the School of Engineering
of the Air Force Institute of Technology
Air Univerity
In Partial Fulfillment of the
Master of Science in Aeronautical Engineering

Larry D. Williams, B.S.
Captain, USAF

December 1985

Acknowledgments

Having endured an intensely laborious stint, I welcome the opportunity to reflect a few words of thanks to those who helped me endure. I thank Dr. Milton Franke and Capt Wesley Cox who as members of my thesis committee and as my professors offered thought provoking suggestions that aided me in formulating this study.

To Dr. William C. Elrod, my principal thesis advisor, I offer thanks for his direction, understanding and invaluable assistance over the past eleven months.

I also thank the technicians at the fabrication shop for their support in preparing the test articles for this study. A special thanks goes to Mr. Jack Tiffany who worked diligently to complete construction of the blower containment chamber, making the cascade facility operational. Without his assistance, this study could not have been completed. Mr. Jay Anderson also deserves mention for his assistance in linking the Scanivalve pressure measurement system to the cascade facility data acquisition system.

Lastly, I thank my wife, Sundra, and daughters, Shawnda and Krista, for their patience, understanding, and tolerance over the last eighteen months.

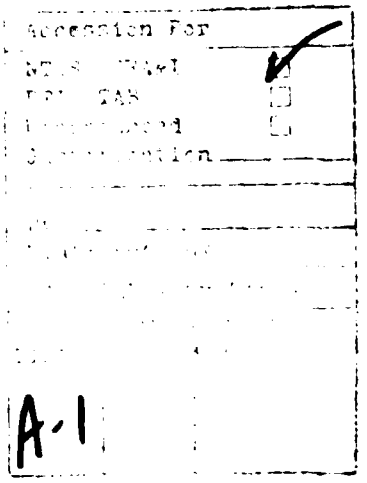

Table of Contents

List of Figures

Page

List of Symbols

Symbol	Name	Units
AA	Arithmetic average roughness	micron
CLA	Center line average roughness	micron
Cp	Coefficient of pressure	
c_p	Specific heat at constant pressure	Btu/lbm-R
dA	Differential area	in^2
dx	Differential length	in
e	Error, least squares curve fit	in
F	Fahrenheit	degree
k	Roughness parameter	micron
ks	Equivalent sand roughness	micron
L	Sample length	in
N	Number of inviscid points	
n	Degree of least squares polynomial	
P	Pressure	lb/in^2
Ra	Average roughness	micron
T	Temperature	°F
U	Velocity	ft/sec
X	Axial direction	in
Y	Vertical direction	in
Z	Lateral direction	in
τ	Ratio of specific heats	
δ	Boundary layer thickness	in
ρ	Density	lbm/ft3
σ^2	Variance	
$\bar{\omega}$	Nondimensional total pressure loss coefficient	

Subscripts

E	Edge
i	Summation index
inv	Inviscid
L	Local
M	Measured
S	Static
0	Total
1	Inlet
2	Exit

Acronyms

AFIT	Air Force Institute of Technology
CTF	Cascade Test Facility
HP	Hewlett-Packard
NACA	National Advisory Committee on Aeronautics
NASA	National Aeronautics and Space Administration
TSI	Thermal Systems International

List of Tables

Abstract

An evaluation of the effects of surface roughness on the pressure distribution and boundary layer over compressor blades in a two-dimensional cascade has been completed. The cascade consisted of seven NACA 65-A506 airfoils with a two inch chord and an aspect ratio of one. The blades were set in the test section at an angle of attack of 15 degrees. The test section unit Reynolds number for the evaluation was in excess of two million per foot.

The changes to the cascade blade pressure distribution were minimal for moderate average roughness (Ra=24.8 microns) to low average roughness values (Ra=.18 micron), except for pressures near the leading edge which were more pronounced. The pressure distribution for a blade surface roughness of 53.8 microns differed considerably from the baseline case.

The cascade test blade experienced laminar separation with turbulent reattachment at moderate to low roughness levels, and fully turbulent flow at high roughness levels. The blade suction surface boundary layer thickness increased with roughness values but was most responsive to the transition from laminar to turbulent flow.

EFFECTS OF SURFACE ROUGHNESS ON PRESSURE DISTRIBUTION AND BOUNDARY LAYER OVER COMPRESSOR BLADES AT HIGH REYNOLDS NUMBER IN A TWO-DIMENSIONAL CASCADE

I. Introduction

Increasing fuel costs over the last decade have prompted operators of military and civil aircraft to seek methods of improving operational efficiency. Decreasing the aircraft fuel consumption rate has been a primary attempt by the industry to cope with the instability in the fuels market.

Considerable attention has been focused on compressor and turbine blade surface quality to achieve increased operating efficiency for turbine engine powered aircraft. Compressor and turbine blade surface quality is a function of two factors, the surface finish on newly manufactured blades and the changes to the original finish incurred through normal use. Military aircraft engines are subjected to solid particle, corrosive gas and liquid ingestion which erode away the compressor blade surfaces. Turbine blades are exposed to combustion by-products which also coat and erode the blade surface.

Because of the multifaceted missions flown by military aircraft, they are more susceptible to the effects of blade

surface imperfections than civil aircraft. Schäffler (Ref. 13) describes three distinctly different flow regimes in the back stages of high pressure ratio military aircraft engines. These flow regimes can be characterized by the following cascade flow boundary layer conditions: laminar separation, turbulent attached flow with hydraulically smooth blade surfaces, turbulent attached flow with hydraulically rough blade surfaces. A hydraulically smooth surface is defined by Schlichting (Ref. 14) as a surface on which the protrusions are so small (or the boundary layer so thick) that they are all contained within the laminar sublayer of the turbulent boundary layer.

Schäffler further established the maximum Reynolds number for laminar separation on a compressor blade at 120 thousand, based on blade chord. Turbulent flow would normally exist above that value.

Compressor rig tests were performed by Bammert and Woelk (Ref. 2) to determine the effects of blade surface roughness on the overall performance of the test compressor. Operating efficiency decreases due to surface roughness ranged up to 13 percent for the roughness values studied. Although full scale rig tests are the principal means of gathering engine component performance data, the test rigs are expensive to operate. Compressor blade cascade testing offers a low cost alternative provided that the cascade test results correlate with those from an actual compressor. Studies by Erwin and

Emery (Ref.7) established that such a correlation exists between two-dimensional cascade data and performance data from test compressors.

Previous studies (Refs. 10, 15) assessed the effects of surface roughness on the overall performance of a two-dimensional cascade of compressor blades in terms of total pressure loss through the cascade. This study was concerned with the effects of surface roughness on the internal flow field of a two-dimensional cascade of compressor blades.

Objective and Scope

The objectives of this investigation were to:

1. Determine the effects of surface roughness on the pressure distribution over compressor blades in a two-dimensional cascade.
2. Determine the effects of surface roughness on the boundary layer growth over the suction surface of compressor blades in a two-dimensional cascade.

NACA 65-A506 airfoils were selected for this study as representative compressor blade profiles. Testing was conducted at the Air Force Institute of Technology (AFIT) Cascade Test Facility (CTF). The CTF has a two inch by eight inch two-dimensional test section which accommodates seven airfoils. The flow field about the center airfoil in the cascade row was the focus of this investigation.

To accomplish the first objective, a NACA 65 series airfoil was instrumented with 28 static pressure taps around its contour at the midspan location. The chordwise locations of the static pressure taps are shown in Figure 1. Metal tubing

was inserted into holes drilled through the end of the test airfoil to locations just below the surface static pressure taps. The metal tubing was used to connect the pressure taps to a Scanivalve pressure measurement system. The instrumented airfoil was placed in the center position of the cascade blade row.

The suction surface boundary layer thickness was measured at six locations from 42.75 to 86.4 percent chord. These locations corresponded to static pressure tap locations along the suction side. The 42.75 percent chord limit was established because of limits in the movement of the hot wire traversing mechanism.

Velocity profiles normal to the blade surface at each location were used to determine the boundary layer thickness, δ, using a procedure outlined by Deutsch and Zierke (Ref.6). The velocity profiles were obtained using hot wire anemometry.

Four surface roughness intensities were included in the study. The surface roughness for each configuration was characterized by average roughness, Ra, and technical roughness, k, defined by Schäffler (Ref. 13:10). Schäffler indicated that Ra alone was not too helpful in defining hydrodynamic characteristics of a surface because a large portion of the smaller roughness elements was fully submerged in the laminar sublayer. The submerged roughness elements are not felt by by the turbulent flow but are included in the Ra measurement measurement. Schäffler's roughness parameter, k, describes the peaks rather than the average roughness.

Schäffler's approach to characterizing surface roughness differed from the traditional scheme. Surface roughness is traditionally measured in terms of equivalent sand roughness, ks. Several relations have been proposed in the literature to relate Ra to ks. Kock and Smith (Ref. 9) proposed that ks was equivalent to approximately 6.2 times Ra. This result was based on profilometer readings from standard grades of sandpaper. Bammert and Sandstede (Ref. 3) proposed that $ks \approx 2.19\,(Ra)^{.877}$. Since a unique relationship between Ra and ks does not exist in the literature, Shäffler's definition was chosen as a second roughness parameter for this study.

The roughness parameters are defined in Appendix A and are shown in Table I. The overall effects of surface roughness on cascade performance were measured in terms of a nondimensional total pressure loss coefficient, $\bar{\omega}$.

TABLE I.

Roughness Data

Conf. No.	Grit Size	Ra(microns)	k(microns)
2	Baseline	0.18	1.6
3	180	19.5	173.6
4	120	24.8	220.7
5	70	53.8	478.8

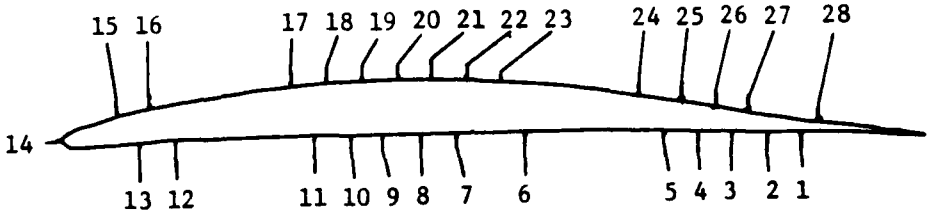

NACA 65-A506

Static Pressure Tap Positions
(percent chord)

1 - 84.75	15 - 6.75
2 - 80.75	16 - 10.75
3 - 76.75	17 - 26.75
4 - 72.75	18 - 30.75
5 - 68.75	19 - 34.75
6 - 52.75	20 - 38.75
7 - 44.75	21 - 42.75
8 - 40.75	22 - 46.75
9 - 36.75	23 - 50.75
10 - 32.75	24 - 66.75
11 - 28.75	25 - 70.75
12 - 12.75	26 - 74.75
13 - 8.75	27 - 78.75
14 - 0.0	28 - 86.4

Figure 1. NACA 65-A506 Test Airfoil

II. Experimental Apparatus

Cascade Test Facility

This investigation was conducted at the Air Force Institute of Technology Cascade Test Facility. The CTF has a test section Reynolds number per foot in excess of two million and an inlet turbulence intensity of less than one percent. Allison (Ref. 1) gives a detailed description of the CTF.

Air for the CTF was drawn into a sealed chamber through a series of screen wire filters and an electrostatic air cleaner by a centrifugal blower. The blower was rated at 40 horsepower with a discharge rating of 3000 cubic feet per minute at a flow pressure increment of 1.66 pounds per square inch. The outlet flow passes through a diffuser section into a stilling chamber where it then passes through a screen/honeycomb flow straightener arrangement. The conditioned air then enters the two inch by eight inch test section.

Test Section

A layout of the CTF's two-dimensional test section is shown in Figure 2. The test section contained a cascade of seven NACA 65-A506 airfoils. The airfoils had a two inch chord length with an aspect ratio of one. The airfoils were set in the test section at a blade row angle of 31 degrees and a stagger angle of 16 degrees. The airfoils were at an angle of attack of 15 degrees, relative to the incoming air flow. The blade turning angle was 19 degrees.

The airfoils at the top and bottom of the blade row were half embedded in the test section wall, simulating an infinite cascade. The blade spacing was 1.333 inches. The solidity based on the two inch chord and blade spacing was 1.5. Solidity is defined by chord length/blade spacing.

Airfoil Configurations

Four configurations of NACA 65-A506 airfoils were investigated. The airfoils were cast from Fiber-Resin Corporation FR-44 casting resin and 5595 amine hardner. The airfoils were made by placing a mixture of the casting resin and hardner in an aluminum casting mold for a 10 hour curing period at room temperature. The casting was then heat treated in two hour increments at 150, 200, and 250 degrees F, respectively, to increase stiffness.

A baseline configuration of hydraulically smooth blades was run for comparison. The other configurations had different levels of surface roughness applied. The roughness was applied from a point just aft of the blade's leading edge to the quarter chord location on the suction side of the blade. Tanis (Ref. 15) found that this roughness configuration caused the greatest losses.

Acrylic sealer was used to glue the different grades of carborundum grit to the blades. A second coat of sealer was applied to the roughened area to minimize dislodgement of particles during testing. The three grades of carborundum used were 180, 120 and 70.

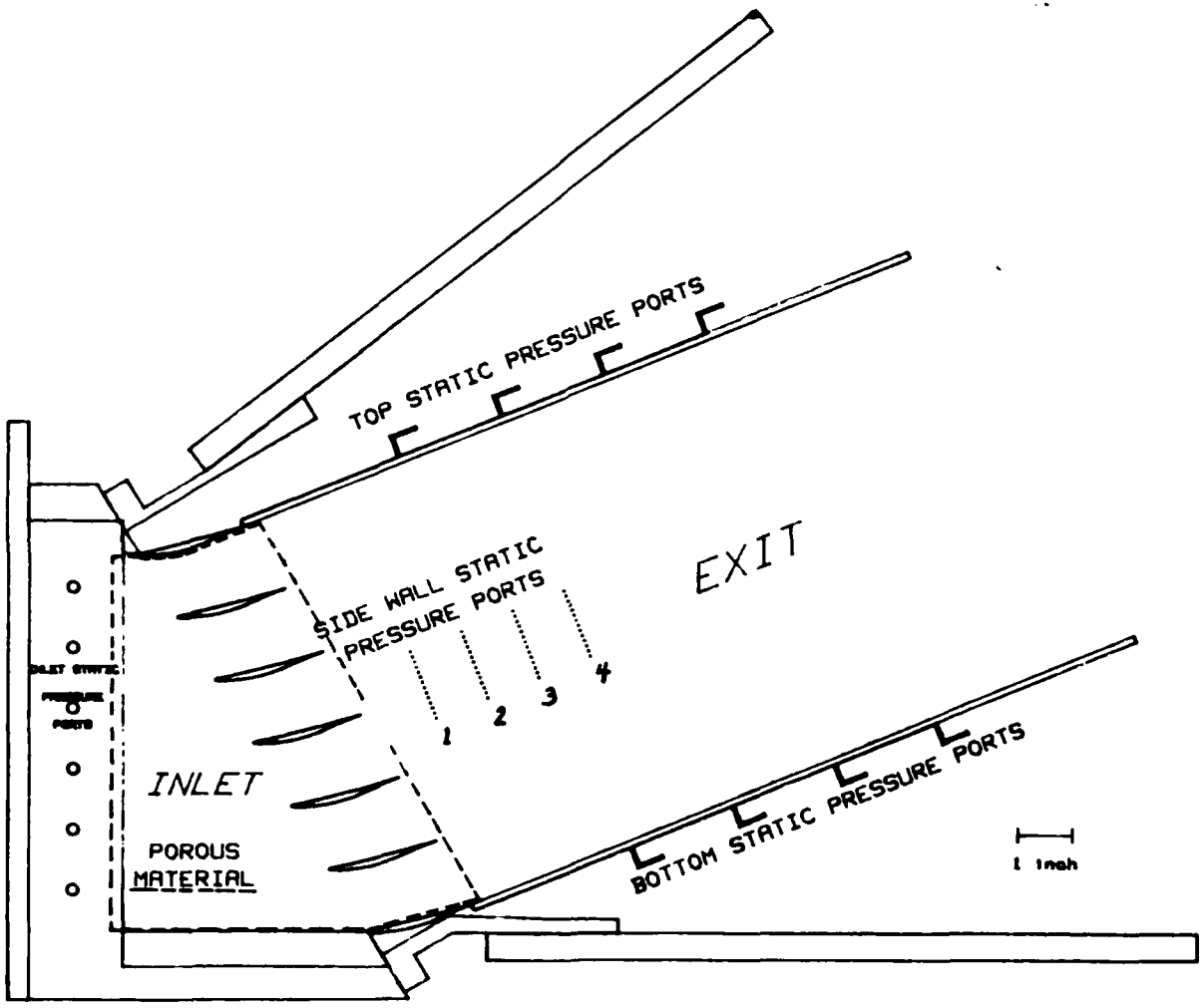

Figure 2. Test Section

The average surface roughness, Ra, was measured with a Rank Taylor Hobson Surtonic 3 profilometer with a parameter and plotter unit attached. Ra was readily obtainable but varied with the sample length and roughness geometry.

Sidewall Suction System

A sidewall suction system was used to reduce boundary layer growth along the test section walls. The system was described in detail by Moe (Ref. 10). Moe found that the sidewall suction system removed a sufficient quantity of the sidewall boundary layer to establish a two-dimensional flow field through the test section.

Exit Diffuser

A two-dimensional diffuser section with adjustable endwalls was attached to the test section. The diffuser was 13 inches long and two inches wide.

The adjustable endwalls permitted the diffuser geometry to be changed to match different flow conditions. Static pressure taps were installed in each endwall and along one sidewall. Proper alignment of the endwalls for this investigation was indicated by endwall and sidewall static pressures approximately equal to ambient.

Instrumentation

Flow conditions in the CTF were monitored by an array of pressure transducers and thermocouples. Three Statham Laboratory P6TC transducers were used to monitor the test section

inlet static, exit total and exit static pressures. A Statham PM60TC and a CEC 4-326 transducer were used to monitor the stilling chamber total pressure and the ambient pressure. Thermocouples were used to monitor the stilling chamber total temperature and the ambient temperature.

A Scanivalve pressure measurement system with a Scanivalve PDCR23D transducer provided a compact 48 channel pressure measurement capability. The system consisted of a model 48S9-3003 Scanivalve, a model CTLR2/S2-S6 controller and a model J102/J104 scanner position display. The system was used to measure the pressure distribution over the surface of the center blade in the cascade.

Each transducer was calibrated over its operating range. A linear curve fit of each calibration was used to convert the electrical output from the transducers to pressures.

Two TSI 1050 hot wire anemometer systems formed an integral part of the flow field instrumentation. A TSI model 1241-10 X-wire hot film probe which was used to survey the velocity profile in the wake region. A TSI model 1218-T1.5 hot wire boundary layer probe was used to obtain the velocity profile over the suction surface of the test blade.

Calibration curves for the X-wire and the boundary layer probes are shown in Figures 3 and 4, respectively. The probes were calibrated over a range of expected operating conditions. The calibration data were collapsed into a single curve by the procedure outlined in (Ref. 15).

Additionally, the CTF had 17 water manometers. Fifteen

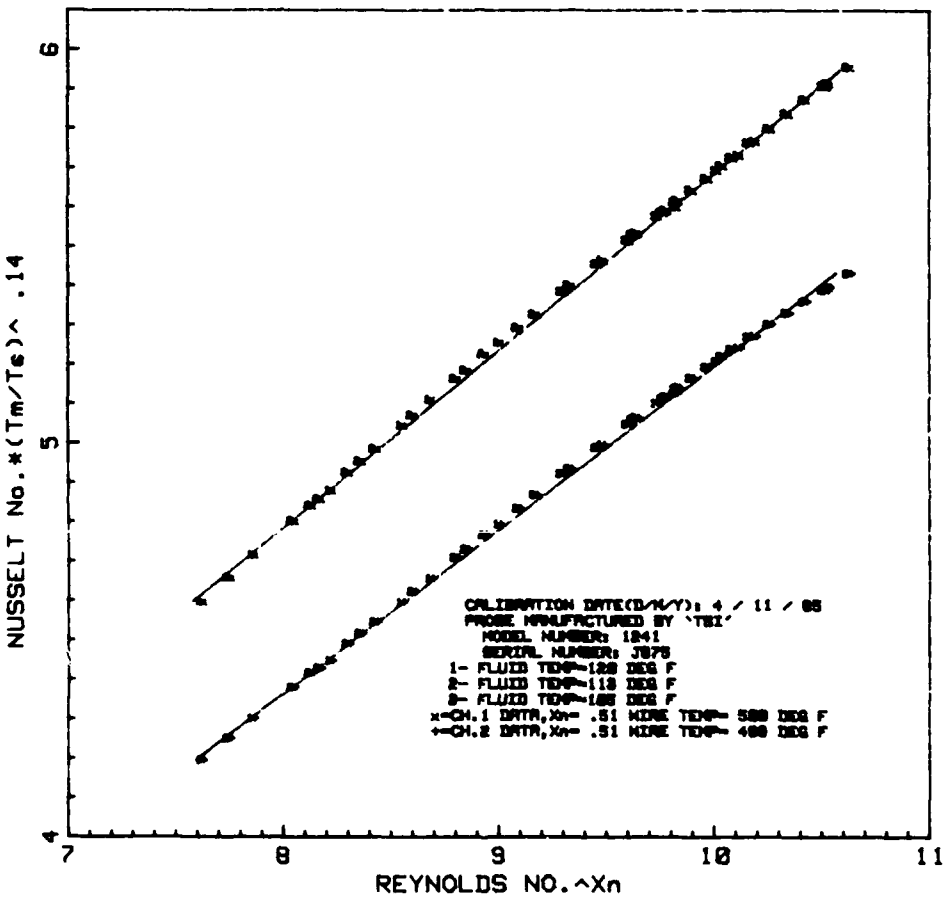

Figure 3. Hot Film Probe Calibration Curve

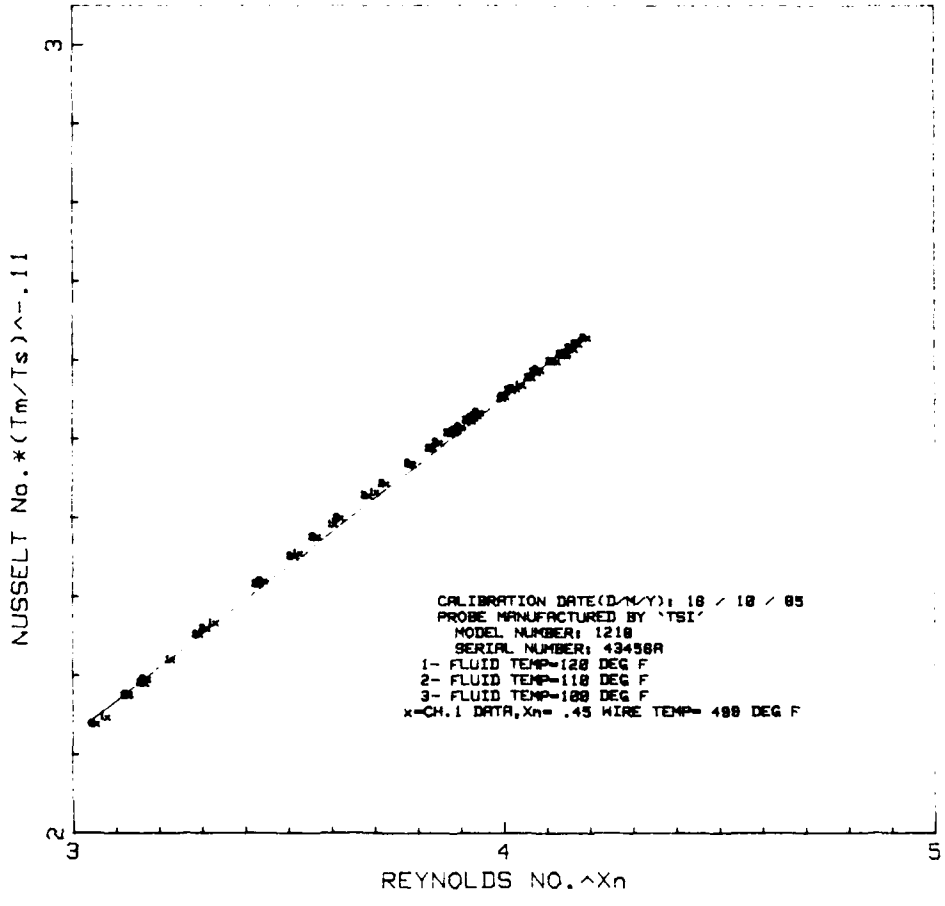

Figure 4. Boundary Layer Probe Calibration Curve

of the manometers were connected to static pressure taps along the test section inlet, sidewalls, and endwalls. These were used to properly align the test section endwalls to insure that two-dimensional flow existed. The remaining two manometers monitored the static pressure in the vacuum supply line for the test section boundary layer control system and the stilling chamber total pressure, respectively.

X-Y Traverser

The CTF was equipped with a traversing system that was capable of motor driven movements in the vertical (Y) and axial (X) planes and could be manually moved in the lateral (Z) plane. The resolution of the digital stepper motors of the traverser system was .001 inch in the Y direction and .002 inch in the X direction. The traverser was integrated into the data acquisition system and could be manually controlled or automatically controlled through the data acquisition system software. The accuracy of the traverser system in the automatically controlled mode was estimated at +/- .002 inches in both the X and Y directions.

Data Acquisition and Processing

The CTF's instrumentation was monitored and controlled by a Hewlett-Packard (HP) 9845B computer and a HP 3052A Automatic Data Acquisition System. The data acquisition system was described in detail by Tanis (Ref. 15).

The data acquisition system was quite versatile. The system had on-line data reduction capability as well as mass

storage capability for electrical signals from the CTF's instrumentation. In the mass storage mode voltage data from the CTF's instrumentation was stored on magnetic disks. The data was later reduced to engineering units. The reduced data was then stored on magnetic disks from which it could be printed or plotted as desired.

III. Procedure and Data Reduction

Testing Procedure

A three phase test program was developed to accomplish the objectives of this investigation. The first phase involved measuring the pressure distribution over the surface of the cascade test blade. The flow field along the suction surface of the cascade test blade was then traversed to obtain boundary layer velocity profiles. Finally, a survey of the cascade wake region was performed to obtain velocity profiles in the wake of the central cascade blade. This series of testing was repeated for each configuration.

Each phase of testing began with an initial CTF run period. The initial run provided time for the test section to reach normal operating temperature (approximately 30-40 degrees F above ambient temperature). After operating temperature was reached, the moveable diffuser endwalls and boundary layer suction were adjusted to balance the test section. The test section was considered balanced when the static pressure distribution across the inlet was uniform and the static pressure along the diffuser walls was approximately equal to ambient pressure. Moe (Ref. 10) demonstrated that the flow field through the balanced test section satisfied the criteria established by Erwin and Emery (Ref. 7) and and by Briggs (Ref. 4) for two dimensional flow. Brigg's cri-

terion of an axial velocity density ratio of one was the measure of two-dimensionality for the test section.

Blade Pressure Distribution. The pressure distribution over the center cascade blade for each configuration was obtained by measuring the static pressure at each of the 28 surface static pressure taps shown in Figure 1. The static pressure profile was measured before each boundary layer velocity profile traverse. These measurements were taken to determine if the effects of blockage by the traverser probe support airfoil were negated by rebalancing the test section after each axial traverser movement.

The test blade pressure data was taken with the Scanivalve pressure measurement system. The discrete pressure measurements were used to calculate the nondimensional pressure coefficient, Cp, at each static pressure tap location.

Blade Boundary Layer Velocity Distribution. The velocity distribution normal to the suction surface of the center cascade blade was measured with a TSI 1218 boundary layer probe installed in the X-Y traverser probe support. The velocity profile was measured at six locations from 42.75 to 86.4 percent chord. The measurement locations were 42.75, 50.75, 66.75, 74.75, 78.75, and 86.4 percent chord. Velocity data was not taken upstream of the 42.75 percent chord location because of the axial movement limitations of the traverser system.

The traverser probe support was aligned parallel to the center cascade blade's mean camber line at the trailing edge.

An angular adjustment routine was included in the data acquisition software to maintain a traverse pattern normal to the local blade surface. The routine calculated the X position required for the Y distance of the probe from the blade surface to maintain a normal traverse pattern. The X position was corrected after each Y traverse increment.

The orientation of the boundary layer probe in the cascade channel is shown in Figure 5. Each traverse consisted of a Y displacement from an initial reference position of approxmately .03 inch in .005 inch increments. The initial reference position was determined by manually moving the boundary layer probe to a position .025 inches from the blade surface at the desired chordwise position. The .025 inch displacement was set using a standard .025 inch thickness gage. The traverser system's X-Y position indicator readings were recorded at the reference position to establish a known reference in the traverser coordinate system. This procedure was repeated at each traverse location. The estimated overall accuracy of the probe positioning procedure was ± .005 inch in the Y direction and ± .004 inch in the X direction.

The reasons for the initial displacement of the probe from the blade surface were twofold:

1. The .03 inch displacement of the probe from the blade surface placed the hot wire probe beyond the region of influence of the wall, for heat transfer purposes. This assumption was based on research by Oka and Kostic (Ref. 11). They found that the cooling effects of a cold wall on a hot wire affected the velocity readings near the surface. The measured velocities in the affected region were as much as five to six times the true value. They established a max-

imum region of influence for the probe tested at one millimeter (.04 inch) at zero flow velocity. The region of influence decreased with Reynolds number, but a definitive relationship was not established.

2. The probe assembly tended to vibrate as the traverser traveled through the boundary layer to its reference position. The vibrations rapidly damped out but were present when the probe was at its closest position to the blade surface. The initial displacement of the probe prevented the likelyhood of the wire contacting the blade surface.

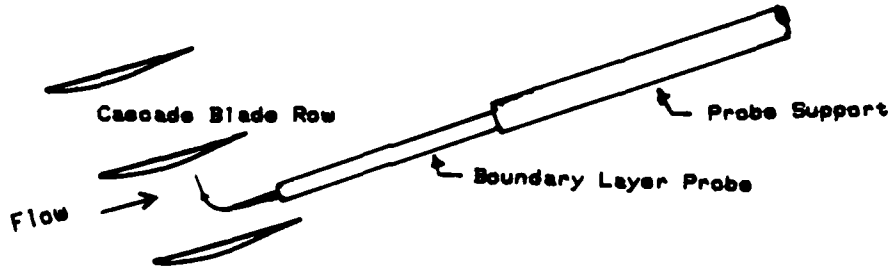

Figure 5. Boundary Layer Probe Orientation

Wake Survey. A survey of the wake region behind the center cascade blade was performed for each roughness configuration. Velocity profiles across the equivalent of one cascade channel were measured at 1.25, 2.25, 3.25, and 4.25 inches downstream of the cascade exit plane. Each traverse consisted of 100 points at .013 inch increments. The velocity profiles were measured with a TSI 1241-10 hot film X-wire probe.

Data Reduction

Blade Pressure Distribution. Blade pressure distribution for each configuration was obtained using a data

acquisition computer program with on-line data reduction capability. The program controlled the data acquisition system scanner and digital voltmeter to sample the test section inlet conditions with each cycle of the Scanivalve pressure measurement system. The program also accessed the CTF's transducer calibration file. This information was used to convert transducer voltage outputs to pressures.

Blade Boundary Layer. The boundary layer along the suction surface of the test blade was calculated from the measured velocity profiles. The procedure used was outlined by Deutsch and Zierke (Ref. 6).

Flow along the suction surface of a compressor blade in a cascade is subjected to a normal pressure gradient which causes the velocity profile to have curvature beyond the boundary layer region. This makes the determination of the boundary layer edge velocity somewhat difficult. Deutsch and Zierke assumed that the measured velocity profile represented a composite velocity profile. The composite profile consisted of a region that was dominated by viscous effects, a region that was inviscid, and a region where the viscid/inviscid flows interacted. The inviscid region was influenced by the normal pressure gradient which resulted in a curved velocity profile, caused by a decrease in the flow velocity as the channel static pressure increased. Thus, the measured velocity profile was composed of an inviscid component, a viscid component (boundary layer velocity profile), and a component that was common to both profiles, the edge velocity.

The edge velocity is equivalent to the free stream velocity in flat plate boundary layer theory.

The composite velocity is expressed mathematically as

$$U_M = U + U_{inv} - U_e \qquad (1)$$

where

U_M = measured velocity
U = boundary layer velocity

U_{inv} = inviscid velocity
U_e = edge velocity

Furthermore, the measured velocity at the wall must go to zero. With the no slip boundary condition for real fluid flow, U must also equal zero at the wall. This indicates that U_{inv} at the wall must equal U_e.

Deutsch and Zierke used an extrapolated quadratic curve fit through a statistical number of points in the inviscid region to determine U_{inv} at the wall. The statistical number of points included in the curve fit was determined by locating a range of points beyond the maximum velocity point where the calculated wall velocity was essentially invariant. N/2 ± N/4 points provided the optimum curve fit, where N is the number of points from the maximum velocity position to the outer edge of the velocity profile.

This procedure was incorporated into one of three data reduction programs used to calculate the boundary layer velocity profile and thus, the boundary layer thickness, δ, which is defined by

$$\delta = y(0.99\ U_\infty) \qquad (2)$$

where

y = displacement from blade surface at U equals $.99U_\infty$

The first program reduced the boundary layer hot wire measurements to velocities. The velocity profiles from each traverse were then processed with a second program which performed a first through fourth order least squares curve fit of the points in the inviscid region. The least squares routine was outlined by Gerald (Ref. 8:468-474, 505-507). The optimum curve fit of the inviscid region was selected using Gerald's criterion of minimum variance, σ^2. The variance for each curve fit was defined by

$$\sigma^2 = \frac{\Sigma e_i^2}{N - n - 1} \qquad (3)$$

where

σ^2 = variance
e_i = error (measured displacement - calculated displacement) at measured velocity
N = Number of points in the inviscid region
n = degree of polynomial

The third program used the equation for the optimum inviscid profile to calculate the boundary layer velocity profile defined by Eq (1). The boundary layer thickness was determined using Eq (2).

Wake Survey. The velocity profile was measured across one equivalent channel width in the wake of the center cascade airfoil. A traverse was taken at 1.25, 2.25, 3.25, and 4.25 inches aft of the cascade exit plane. The hot wire

measurements were converted to velocity values based on the hot film probe calibration curve shown in Figure 3.

The velocity profiles were processed by a second computer program to yield the nondimensional total pressure loss coefficient. The measured velocity profiles were corrected for previously observed hot film probe errors (Refs. 10, 15) which indicated that velocities were two to five percent above velocities obtained using a pitot-static probe.

The exit plane total pressure and the nondimensional total pressure loss coefficient are defined by the following equations:

$$P_{o2} = P_2\left(1 + \frac{V_2^2}{2C_pT_{o2}} \right)^{\gamma/(\gamma - 1)} \tag{4}$$

$$\bar{\omega} = \frac{P_{o1} - \bar{P}_{o2}}{1/2 \quad V_1^2} \tag{5}$$

where

P_{o1} = inlet total pressure
$\bar{P}_{o2}$ = mass averaged exit total pressure
$1/2\ \rho V_1^2$ = inlet dynamic pressure
T_{o1} = inlet total temperature

The mass averaged exit total pressure is calulated by

$$\bar{P}_{o2} = \frac{\int P_{o2}\, \rho V2\, dA}{\int \rho V_2\, dA} \tag{6}$$

IV. Results and Discussion

Two configurations of NACA 65 series test blades were instrumented with static pressure taps. One blade had all pressure taps aligned along the blade centerline. The other blade had alternating taps with every other tap offset by 1/8 inch from the centerline. The two blades were evaluated to determine if the alignment pattern of the static pressure taps influences the measured pressures. The calculated nondimensional pressure coefficient, Cp, profiles for the two blades are shown in Figure 6. The profiles were essentially identical in the region where the pressure taps were closely spaced, chordwise. The indicated pressure coefficient at the trailing edge, 100 percent chord location, was computed as the arithmetic average of the last measured aft suction and pressure surface values.

The blade with the aligned pressure taps was used for the study. Because of difficulty in producing instrumented blades, a single blade was used for all four test configurations. Roughness elements were removed from the test blade blade after each configuration was tested. Carborundum grit for the next configuration was then applied.

Two-dimensional flow through the test section was maintained by adjusting the diffuser endwalls and the test section boundary layer control suction. The test section was rebal-

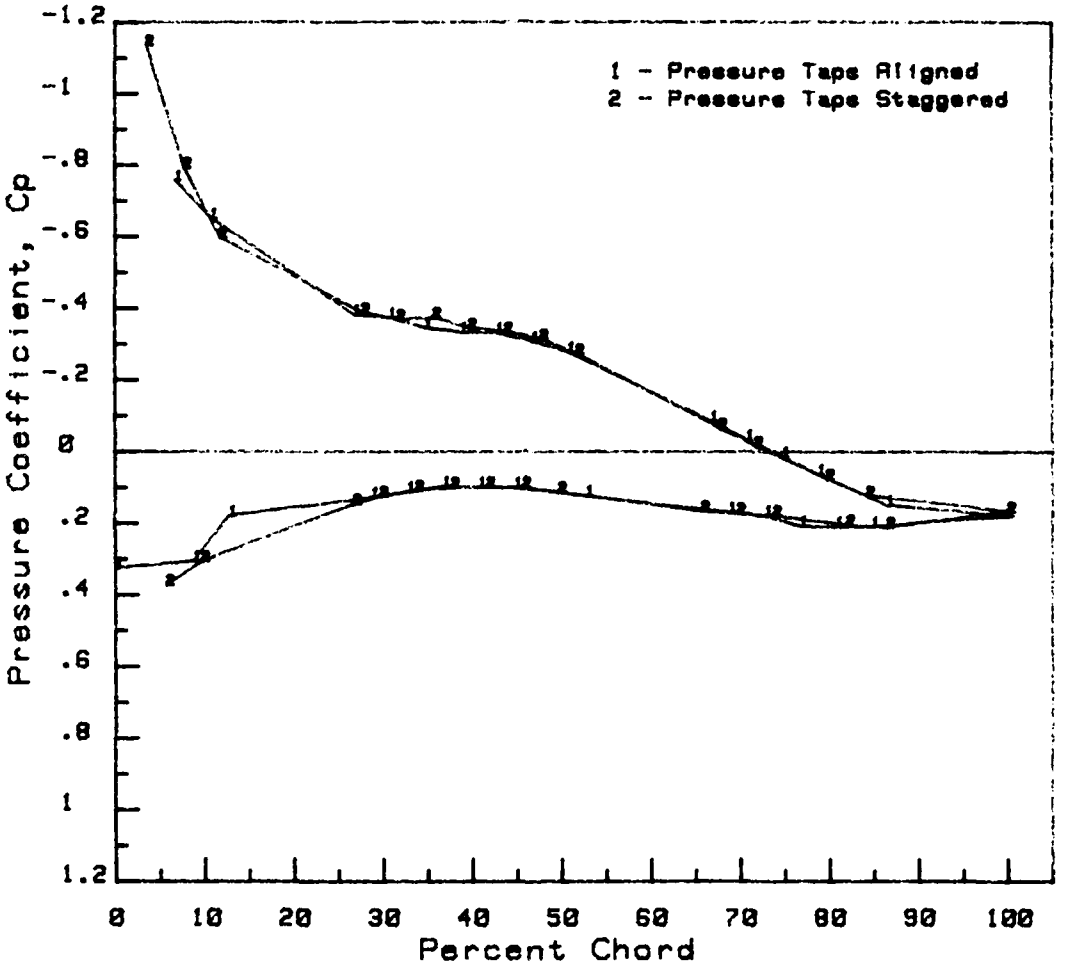

Figure 6. Blade Pressure Tap Alignment Evaluation

anced after the traverser was moved to another chordwise traverse location.

Blade Pressure Coefficient

The static pressures along the test blade surface were used to calculate the nondimensional pressure coefficient at each pressure tap location along the blade midspan contour. Cp is defined as

$$Cp = \frac{P_t - P_s}{1/2\ \rho V_1^2} \qquad (7)$$

The local blade static pressure (P_L) was also required to reduce hot wire boundary layer probe measurements to velocity values. Therefore, pressure profiles were obtained at each traverse location for each of the four test configurations. The Cp plots at each traverse location were essentially identical for a particular blade roughness. This indicated that the flow field through the cascade blade row did not change for the different traverse positions.

Average pressure profiles for configurations 2 thru 5 are shown in Figures 7 thru 10, respectively. The suction surface pressure profiles for configuration 2 thru 4 showed a characteristic flat region. Cebeci (Ref. 5) described flat spots in pressure profiles as separation zones. The flow for configurations 2 thru 4 appeared to separate at approximately 34.75 percent chord then reattach before the

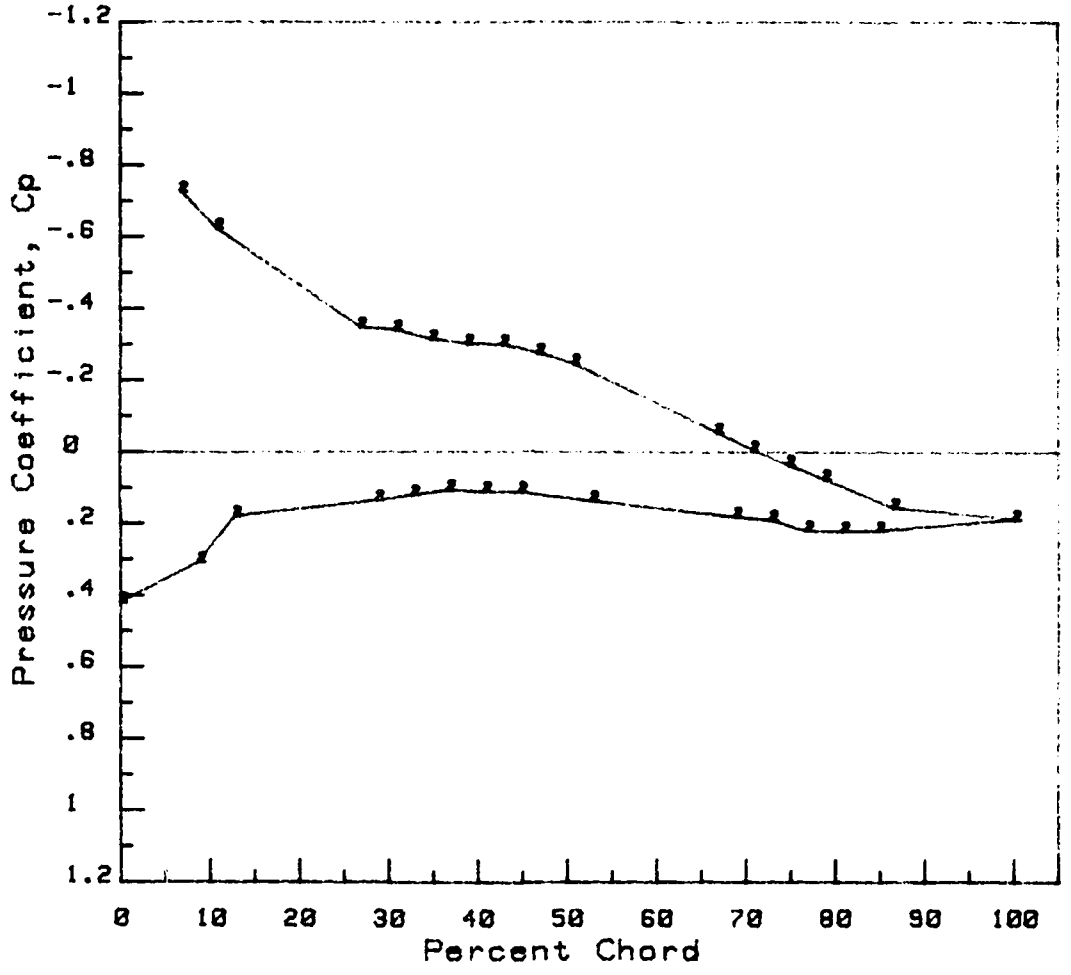

Figure 7. Pressure Profile, Conf. No. 2, Ra=.18 micron

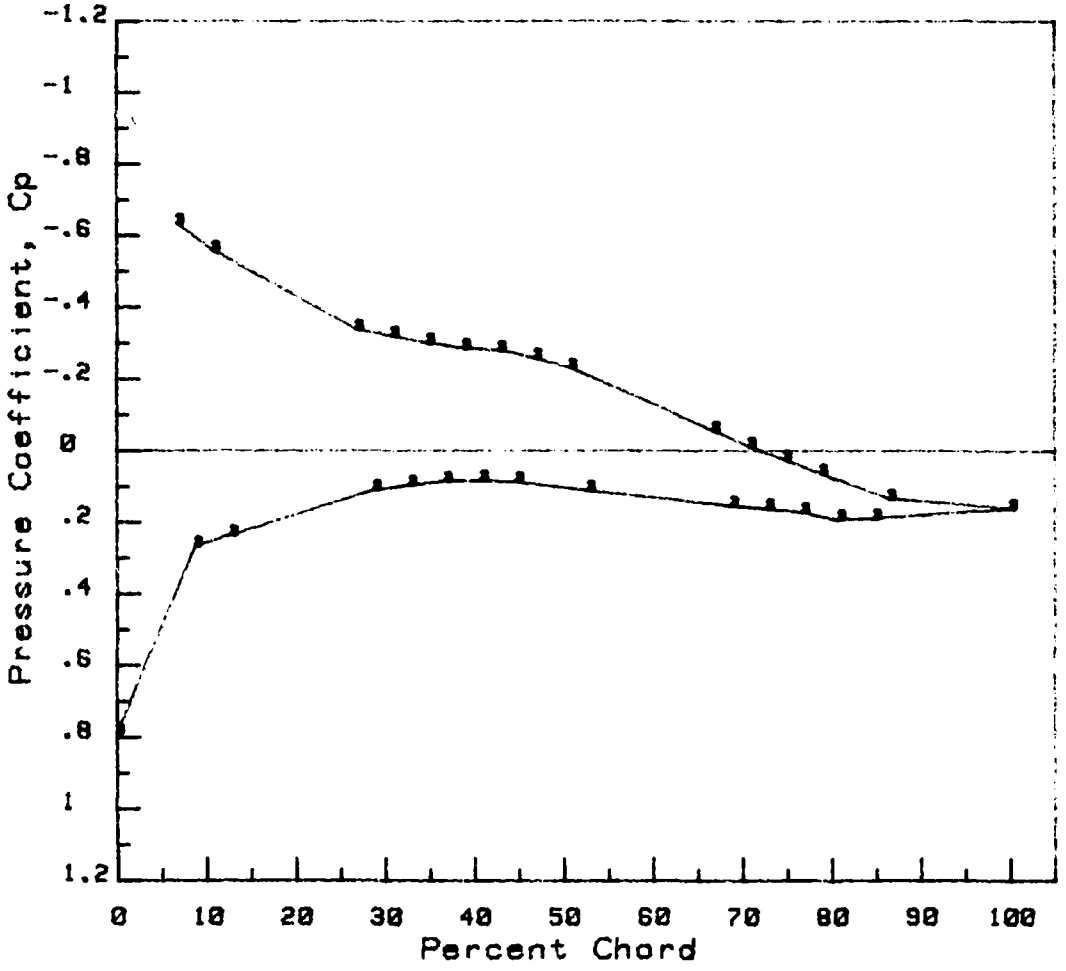

Figure 8. Pressure Profile, Conf. No. 3, Ra=19.5 microns

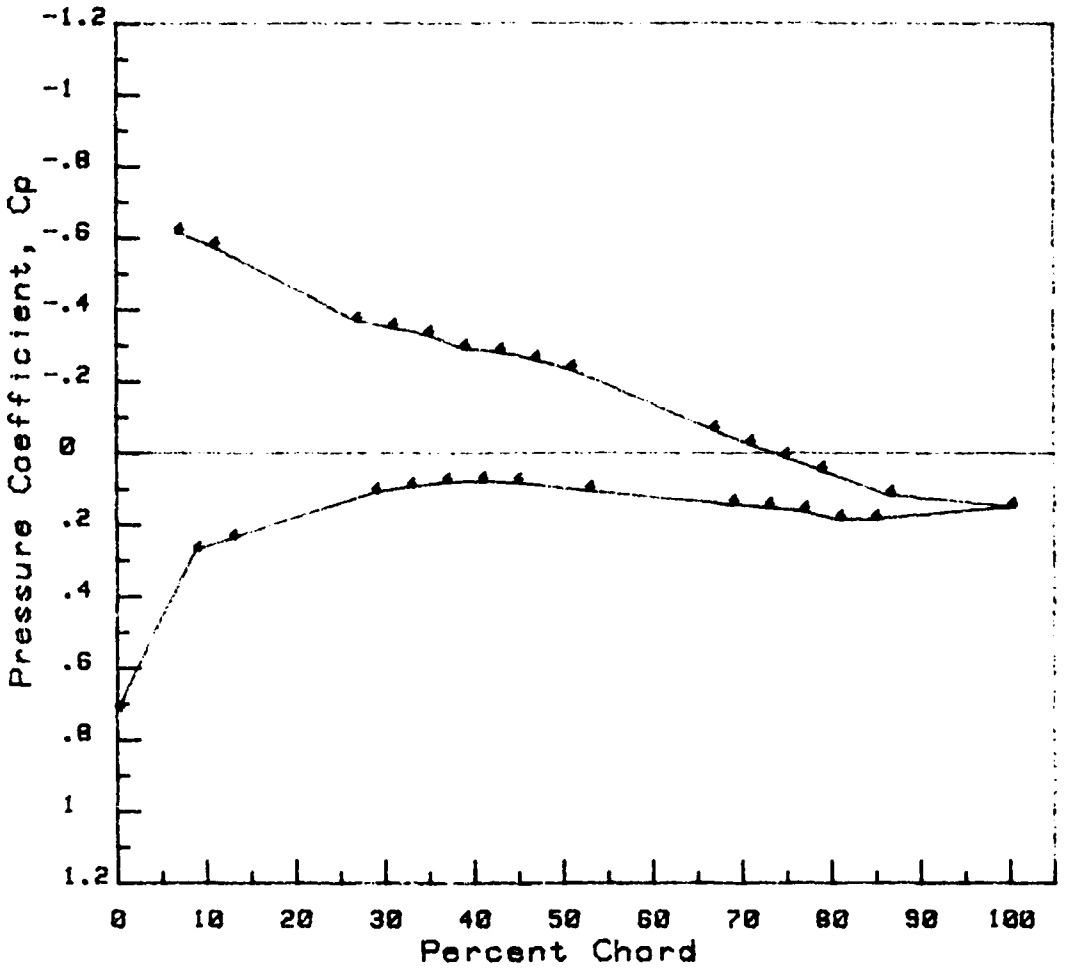

Figure 9. Pressure Profile, Conf. No. 4, Ra=24.8 microns

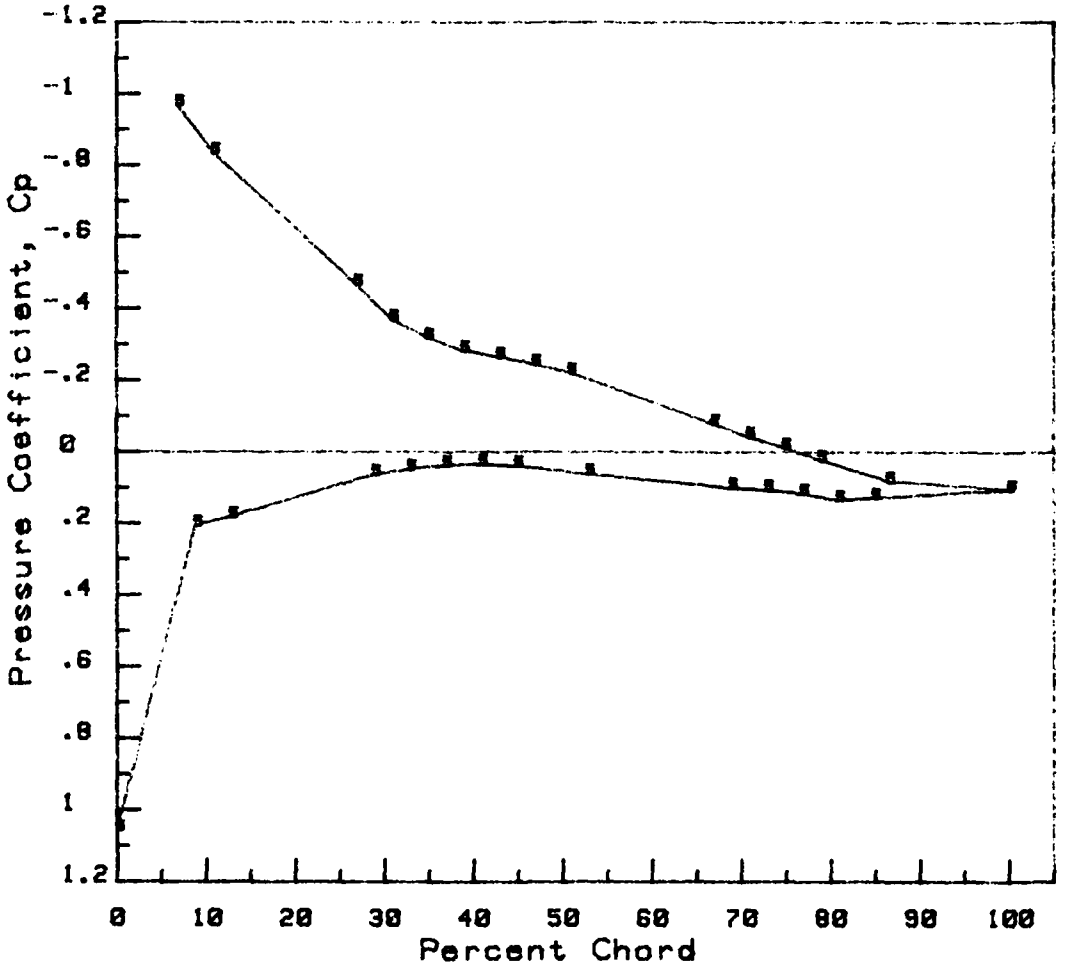

Figure 10. Pressure Profile, Conf. No. 5, Ra=53.8 microns

42.75 percent chord location in configuration 3 and 4 and by 46.75 percent chord in configuration 2.

The occurrence of separation bubbles was also noted by Saxena (Ref. 12) for similar flow conditions. Saxena noted flow separation with reattachment for smooth blades and blades with roughness from the leading edge to 10 and 20 percent chord, respectively, for a NACA 65 (21) 10 compressor blade cascade. The test section chord Reynolds number for Saxena's data was of the same order of magnitude as that for this investigation.

The pressure coefficient near the leading edge of the suction sides of configurations 3 and 4 increases from the baseline value, with Cp for configuration 4 being slightly higher than for configuration 3. This is consistent with results for cascade flow using blades with increasing surface roughness observed by Saxena.

The pressure profile for configuration 5 was different from the other three configurations. The suction surface pressure was 25 percent lower than the baseline configuration near the leading edge. The pressure side leading edge pressure was 1.6 times the baseline value. Except for the pressure side leading edge region, the pressure coefficients were generally lower around the contour than for the other configurations. The separation bubble apparent in the data for the other three configurations was not visible in this case. Turbulent flow appeared to exist over the entire suc-

tion surface unless a separation bubble occurred in the region from 15 to 25 percent chord which did not have pressure taps.

Blade Boundary Layer

The suction surface boundary layer thickness, δ, was determined from 42.75 to 86.4 percent chord for each roughness configuration using Eq (2). The boundary layer velocity profiles were calculated using Eq (1). The optimum Uinv profile was calculated using N/2 of the outermost points of the measured velocity profile. The U_{inv} profile was obtained using the optimum first or second order least squares curve fit, based on Gerald's criterion (Ref. 8) for the optimum fit. The velocity profiles obtained during this investigation did not exhibit as much curvature as the profiles measured by Deutsch and Zierke (Ref. 6) because of the differences in airfoil shape and traverse length.

Plots of the composite velocity profiles at each traverse location for configuration 2 are shown in Figures 11 through 16. Each figure has a plot of the measured velocity profile, a curve fit of the inviscid velocity profile, and the calculated boundary layer velocity profile. The indicated edge velocity is equivalent to the free stream velocity in flat plate boundary layer theory. Plots for the other configurations are shown in Appendix B. The shape of the boundary layer profiles was essentially constant for all of the plots, indicating that similar flow conditions were pre-

sent in the surveyed region for all roughness values tested. The boundary layer parameters at each traverse location for all configurations are shown in Table 2. The calculated velocity based on the measured local static pressure (U_m) at each traverse is also included in Table 2. For the surveyed portion of the suction surface, the values of U_m and U_e were approximately equal when the blade channel static pressure gradient was essentially constant. This position corresponded to the 42.75 percent chord location for this investigation. Deutsch and Zierke's (Ref. 6:30) data showed a similar trend for the values of U_m and U_e.

A plot of boundary layer thickness as a function of chordwise location for each configuration is shown in Figure 17. The boundary layer thickness increased with increasing roughness, but did not follow any dedectable trend. Boundary layer growth was also indicated qualitatively by the number of points in the boundary layer velocity profile with a magnitude less than U_e, since the initial sensor displacement from the blade surface was approximately equal for the data being compared. The largest change in δ for a given traverse location was between configurations 2 and 3, although the largest change in roughness was between configurations 4 and 5. The smallest change in δ was between configurations 3 and 4.

The boundary layer for each roughness configuration had a region where the change in δ from one traverse location to the next was minimal. The regions were from 66.75-74.75 percent

chord for configuration 2, 74.75-78.75 percent chord for configurations 3 and 4. This investigation did not establish a reason for the occurrence of these regions. However, they appeared just beyond the transition to turbulent flow for configurations 2, 3, and 4.

Figure 18 is a plot of the boundary layer edge velocity as a function of chordwise position. The suction surface boundary layer edge velocity decreased at a nearly constant rate with increasing roughness except for configuration 5. U_e's rate of decrease for configuration 5 changed at approximately 50.75 percent chord. Beyond that point the slope of the U_e curve decreased, resulting in values of U_e higher than those for the other roughness values at traverse locations near the trailing edge.

Figure 19 is a plot of the boundary layer velocity profile for configuration 5, 74.75 percent chord, taken on two different test days. The closeness of the profiles indicated that the testing technique for this investigation produced repeatable results.

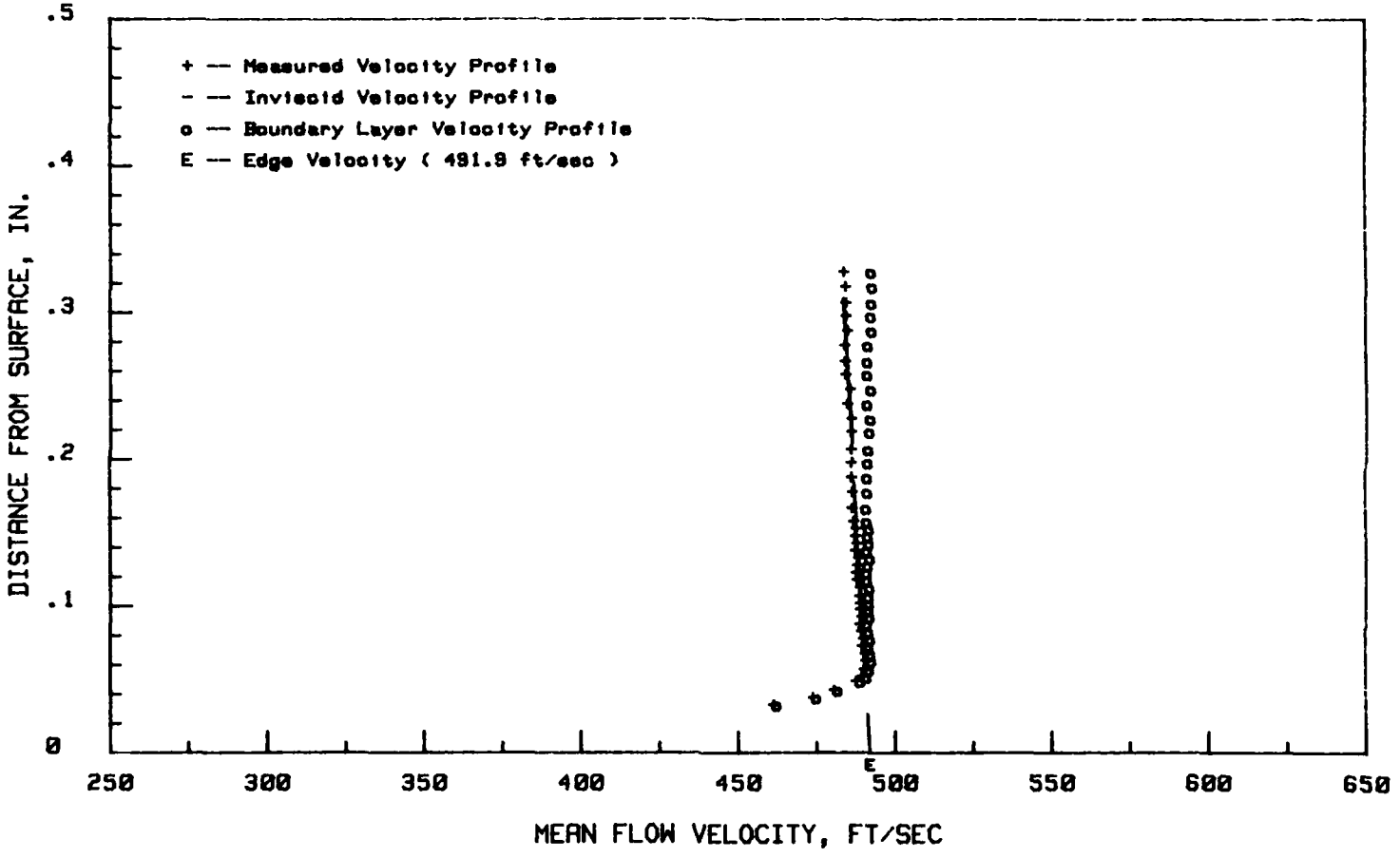

Figure 11. Boundary Layer Velocity Profile, Conf. No. 2, 86.4 Percent Chord: Ra=.18 micron

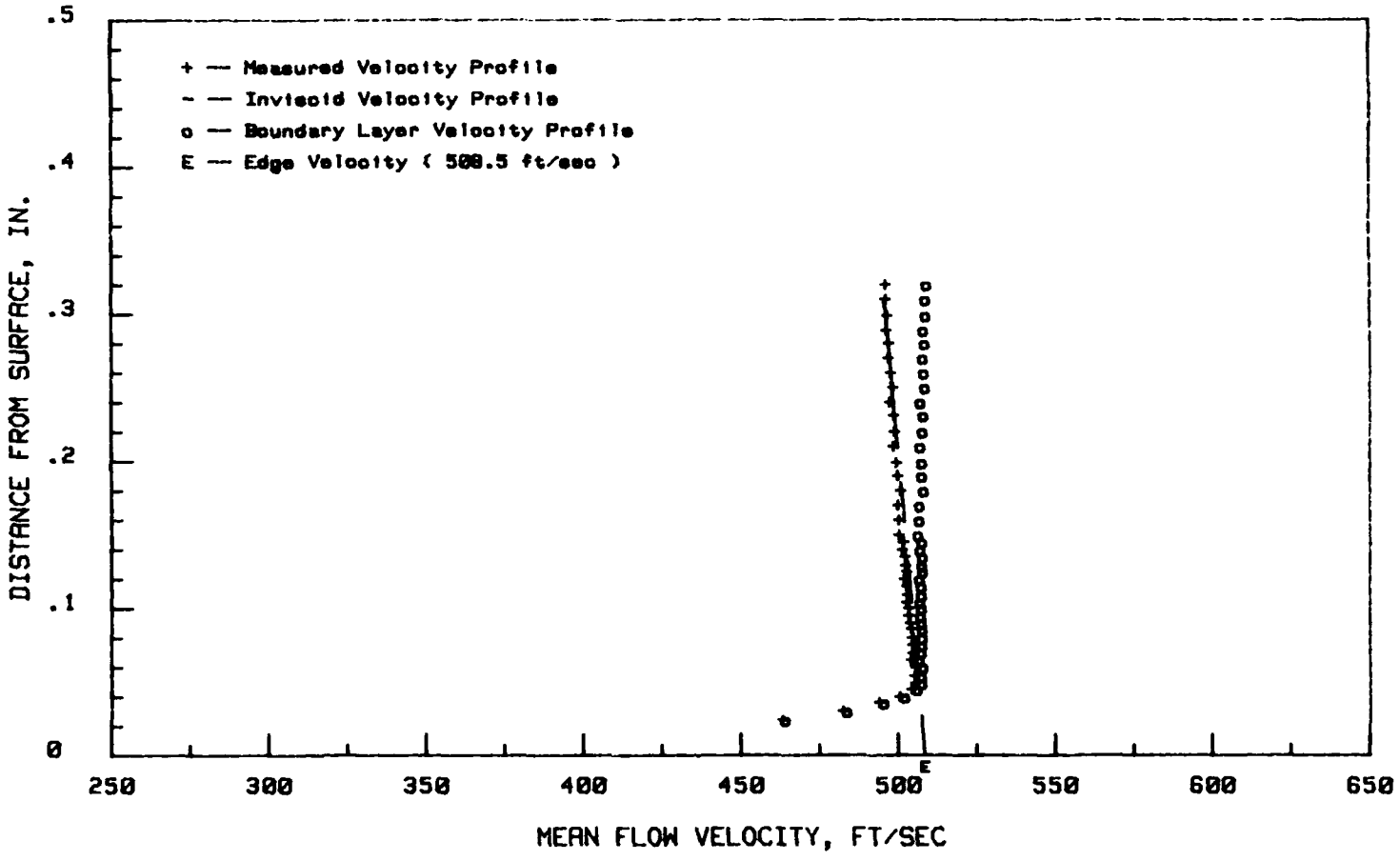

Figure 12. Boundary Layer Velocity Profile, Conf. No. 2, 78.75 Percent Chord: Ra=.18 micron

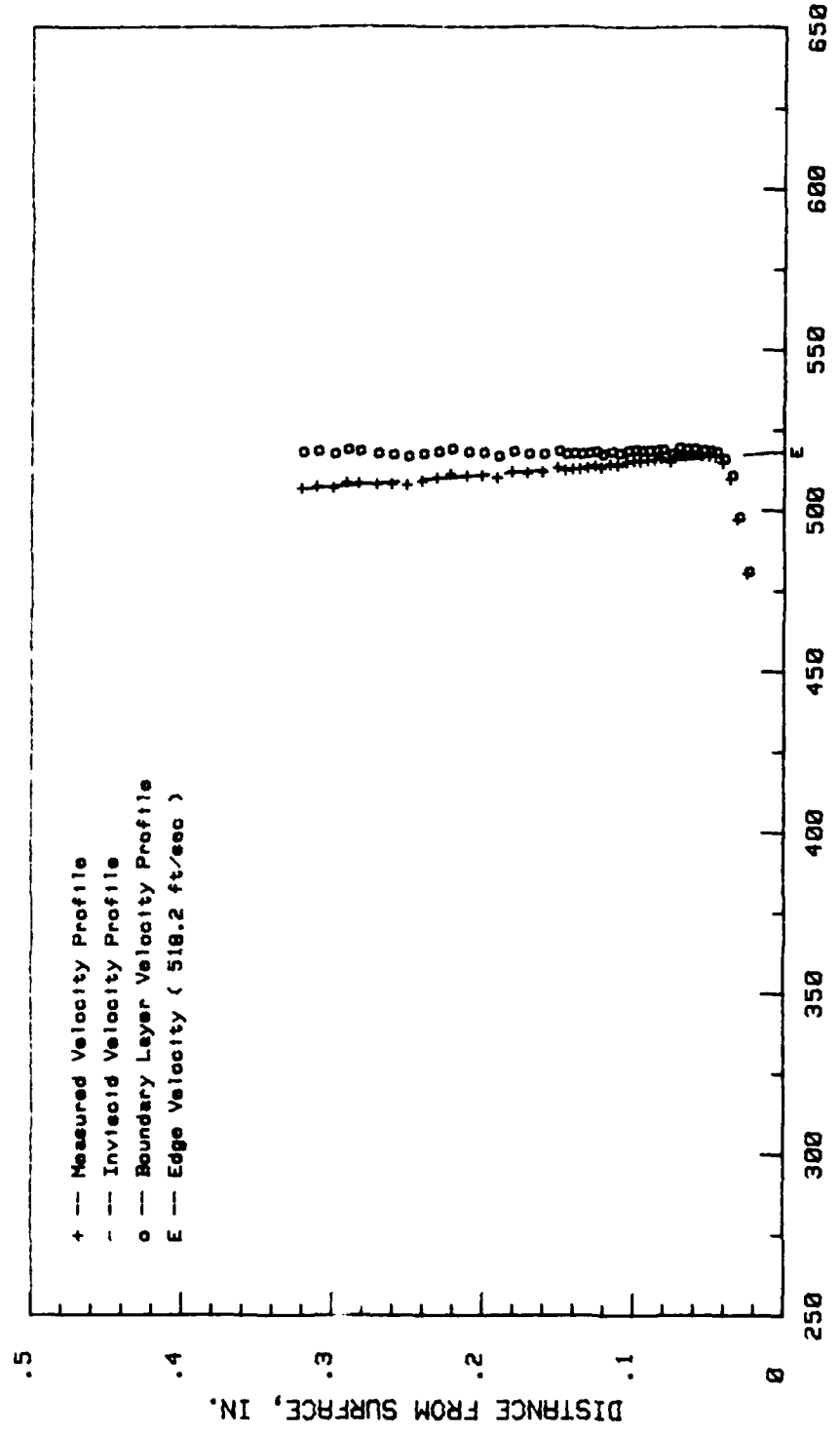

Figure 13. Boundary Layer Velocity Profile, Conf. No. 2, 74.75 Percent Chord: Ra=.18 micron

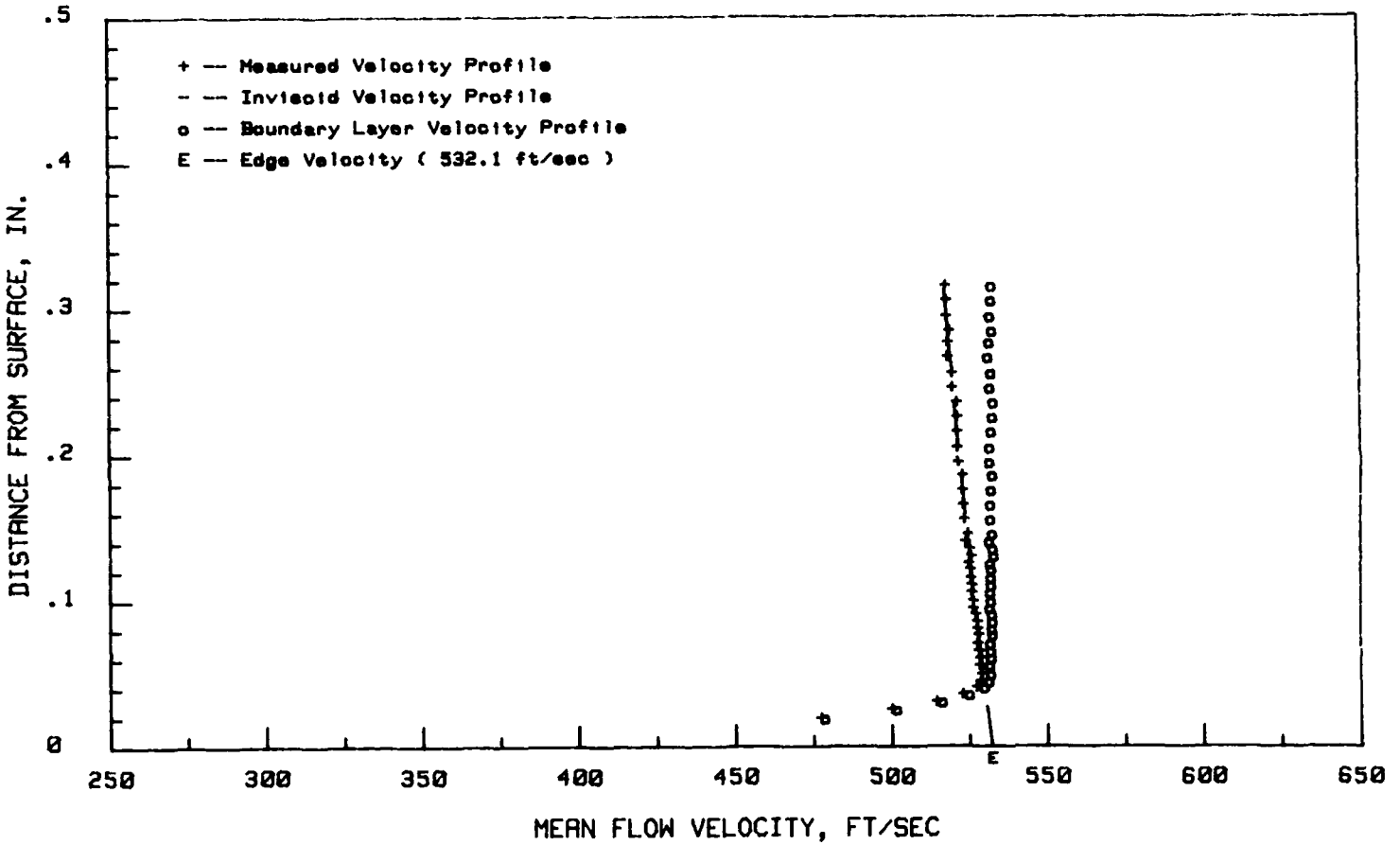

Figure 14. Boundary Layer Velocity Profile, Conf. No. 2, 66.75 Percent Chord: Ra=.18 micron

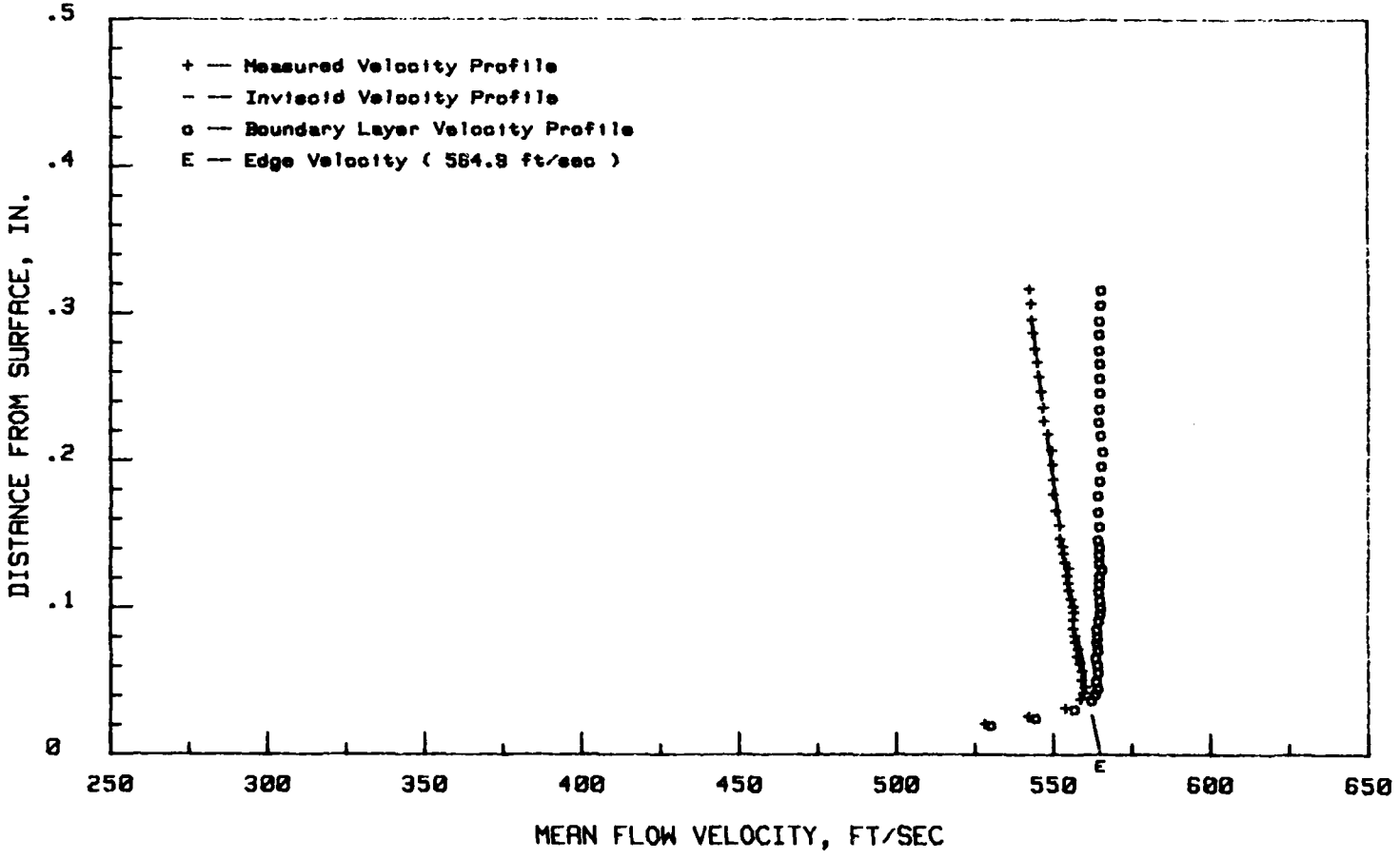

Figure 15. Boundary Layer Velocity Profile, Conf. No. 2, 50.75 Percent Chord: Ra=.18 micron

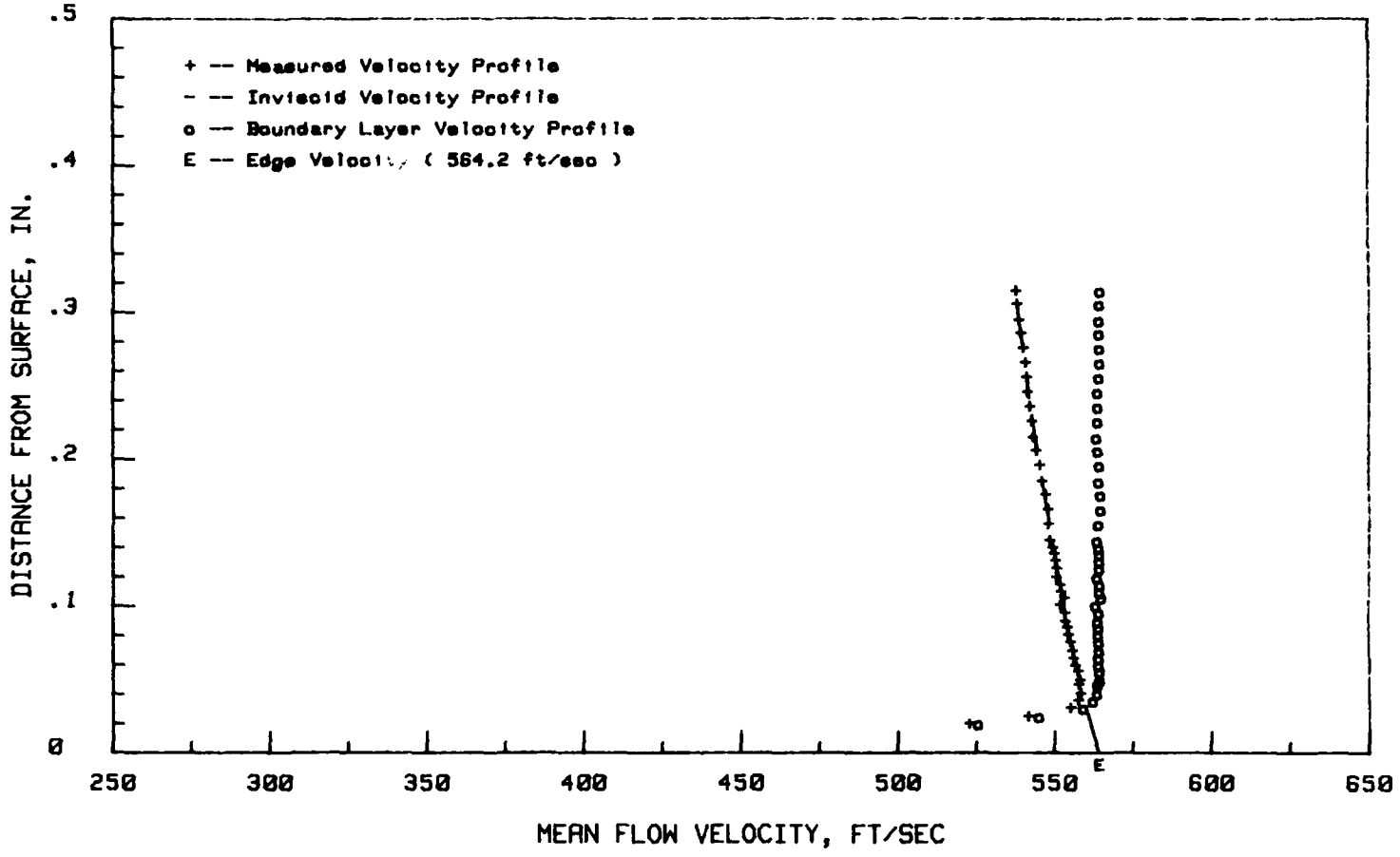

Figure 16. Boundary Layer Velocity Profile, Conf. No. 2, 42.75 Percent Chord: Ra=.18 micron

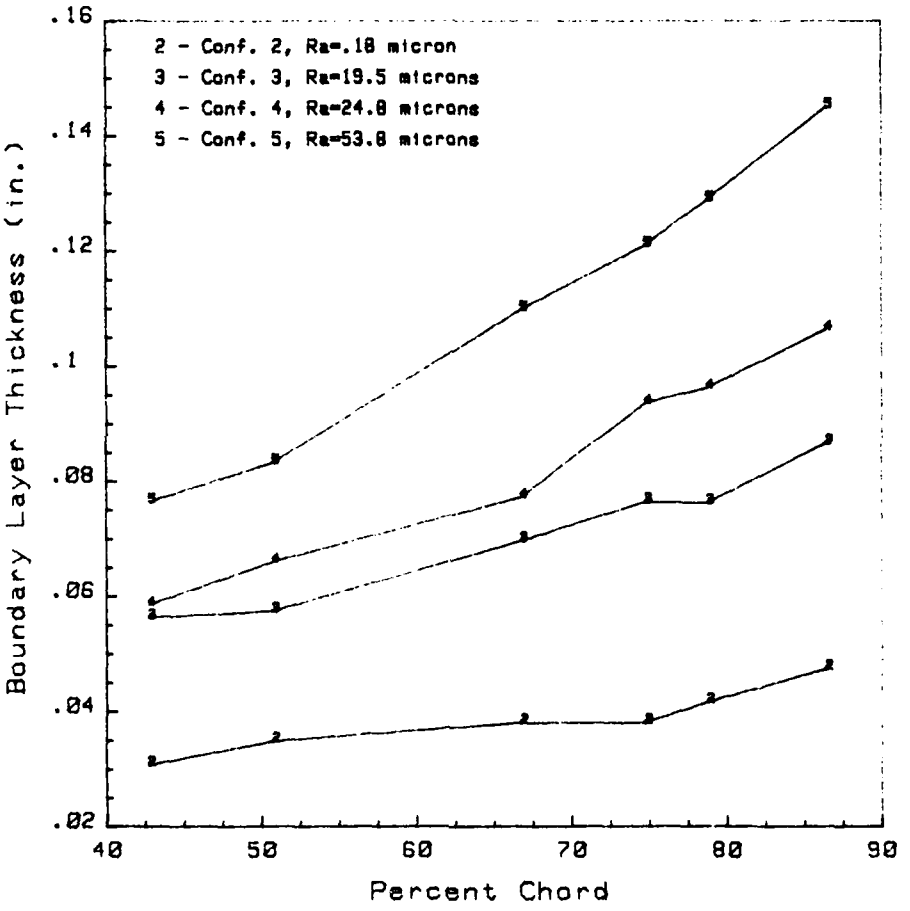

Figure 17. Boundary Layer Thickness, δ

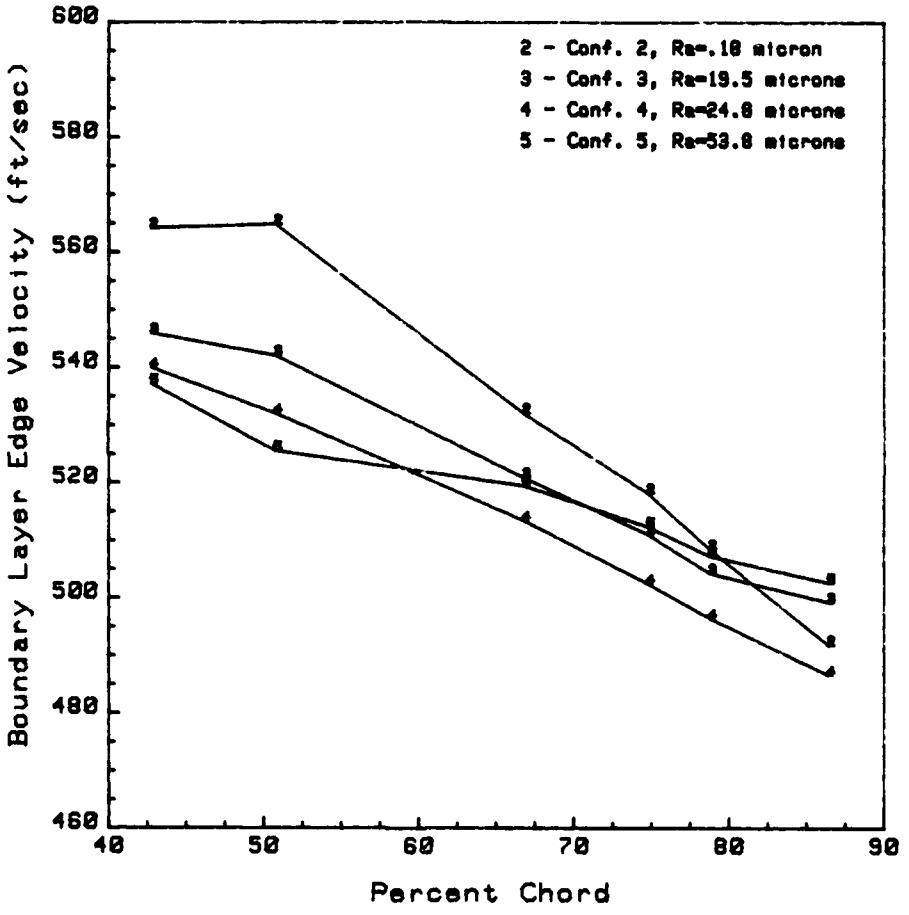

Figure 18. Boundary Layer Edge Velocity

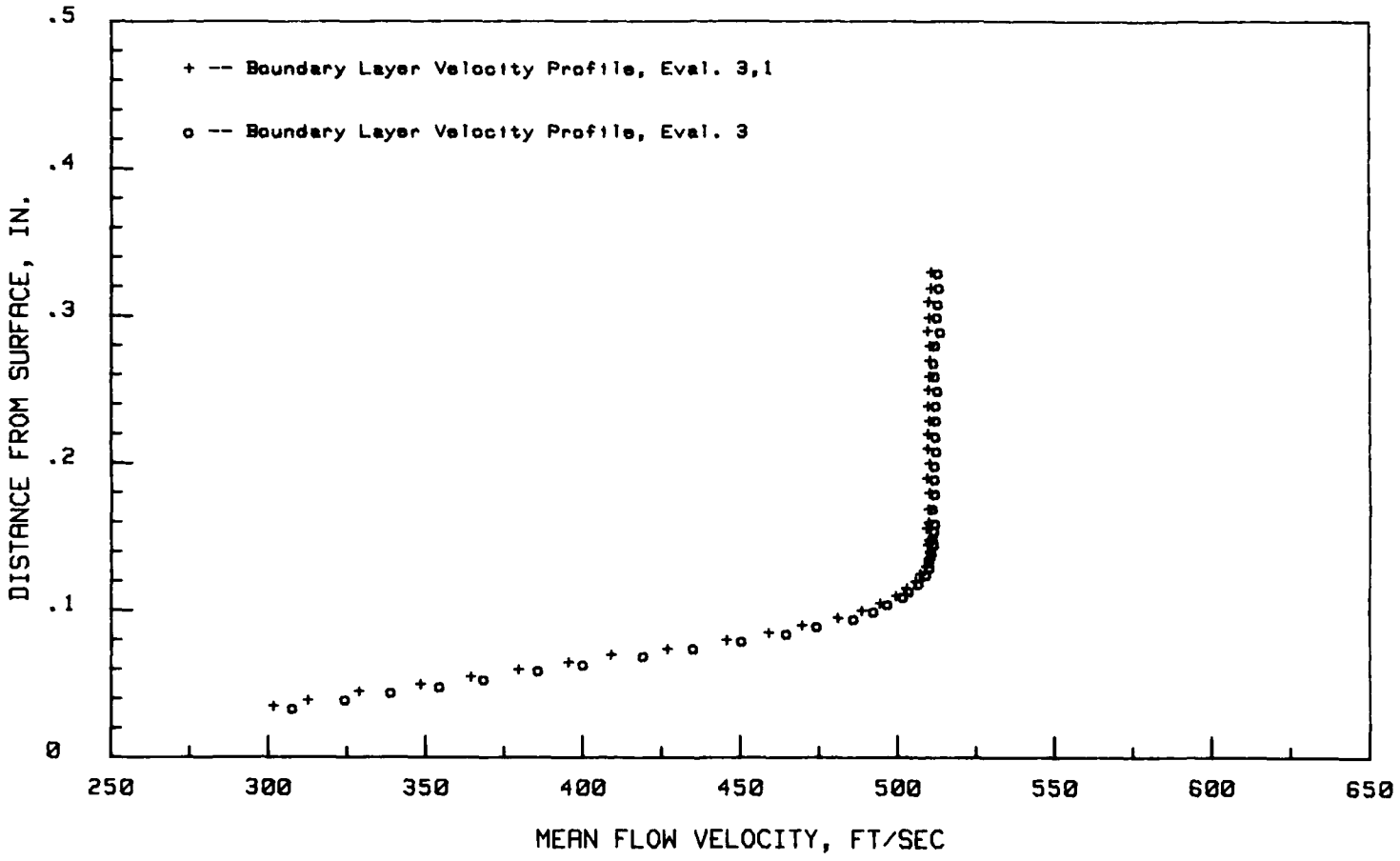

Figure 19. CTF Repeatability Evaluation, Conf. No. 5, 74.75 Percent Chord: Ra=53.8 microns

TABLE II

Blade Boundary Layer Parameters

Conf. No.	Traverse Position (percent chord)	U_∞(fps)	U_e(fps)	δ(in)
2	86.4	472	492	.047
	78.75	489	509	.042
	74.75	499	518	.038
	66.75	507	532	.038
	50.75	541	565	.035
	42.75	547	564	.031
3	86.4	463	499	.087
	78.75	489	504	.076
	74.75	486	511	.076
	66.75	504	521	.070
	50.75	534	542	.057
	42.75	542	546	.056
4	86.4	463	487	.106
	78.75	477	497	.096
	74.75	486	503	.094
	66.75	502	514	.077
	50.75	534	532	.066
	42.75	541	540	.059
5	86.4	475	503	.145
	78.75	488	507	.129
	74.75	496	512	.121
	66.75	509	520	.11
	50.75	536	526	.083
	42.75	544	537	.074

Wake Survey

Schlichting (Ref. 14) indicated that a determination of losses through a cascade require three separate partial calculations.

1. Determination of the pressure distribution over each blade contour.
2. Calculation of the boundary layer at the blades.
3. Determination of the losses due to mixing in the wake behind the cascade.

In this study the pressure distribution and a partial boundary layer map for the center blade in the cascade were measured. However, a method for determining the mixing losses was not evident. Therefore, the nondimensional total pressure loss coefficient determined from blade wake surveys by Eq (4-6) was used to quantify the overall cascade performance.

The measured value of $\bar{\omega}$ for configurations 2 thru 5 were .051, .0525, .0551, and .0808, respectively. The difference between the values of $\bar{\omega}$ for configurations 2, 3, and 4 was small in comparison to the difference in roughness value.

Roughness values for configurations 2 thru 4 are relatively close to those tested by Moe (Ref. 10). Moe reported $\bar{\omega}$'s of .0387, .044, and .0483 for his equivalent roughness configurations. Examination of Moe's data revealed a discrepancy in the mass flow calculation. Corrected values of $\bar{\omega}$ for Moe's first and third cases were .0428 and .0534. The .0534 value was comparable to the .0551 value obtained for configuration 4 of this study. Because of the difference in the loss coefficient for configuration 2 and Moe's baseline case, an additional evaluation was performed in which the test blade was replaced with a smooth blade (Ra=.07 micron) without pressure taps. A loss coefficient of .045 was obtained. This value was comparable to Moe's baseline loss coefficient.

The .11 micron increase in Ra from the smooth blade to the baseline (configuration 2) test blade resulted in a 13 percent increase in $\bar{\omega}$. As the surface roughness was in-

creased from the baseline roughness (Ra=.18 micron) to that of configuration 3 (Ra=19.5 microns), configuration 4 (Ra=24.8 microns), and configuration 5 (Ra=53.8 microns), the loss coefficient increased by 2.9, 8.0, and 38.4 percent, respectively.

V. Conclusions and Recommendations

Conclusions

The pressure distribution over the centerline contour of the central cascade blade and the suction surface boundary layer profile from 42.75 to 86.4 percent chord were investigated. Analysis of the data taken over the course of the study yielded the following conclusions.

1. From the pressure profiles, it appeared that laminar separation with reattached turbulent flow occurred on the cascade blades for moderate (Ra=24.8 microns) to small (Ra=.18 micron) roughness values. The point of reattachment moved toward the leading edge with increasing roughness.

2. Increasing surface roughness causes a decrease in the boundary layer edge velocity.

3. The effects of increasing surface roughness on the nondimensional total pressure loss coefficient are significant at small roughness values. As roughness values increase, a range of values exist that have minimal effects on the loss coefficient. Higher roughness values produce further significant increases in the loss coefficient.

Recommendations

If cascade testing is to be validated as an alternative to full scale component rig testing, flow conditions in the cascade must be similar to those in the actual component. Since the turbulence levels for actual engine compressors are considerably higher than those experienced in the CTF, a study of the effects of varying the test section inlet turbulence level on the cascade performance would be of value.

The suction surface boundary layer thickness over the rear half of the test blade was investigated in this research. A more detailed investigation should be directed toward the region of the apparent separation. Such a study should explore the dynamics of the flow field in the separation zone and performance gains attainable by treating the separation problem.

APPENDIX A: Roughness Definition

The arithmetic average surface roughness, Ra, is defined by Schäffler (Ref. 13:10) as

$$Ra = AA = CLA = 1/L \int_L |Y| \, dx \qquad (8)$$

Ra is normally obtained with a profilometer or similar instrument that moves a stylus across the surface of the test material. The stylus displacements are sensed electrically and are integrated over the traverse length to yield Ra. The average roughness is measured in micrometers (microns) or microinches. Figure 18 shows a typical surface roughness trace and a definition of Ra.

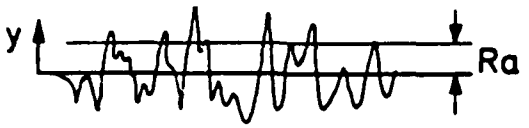

Figure 18. Average Surface Roughness, Ra

Schäffler's roughness parameter, k, is the arithmetic mean of the 10 highest peaks (millimeters) minus the arithmetic mean of the 10 deepest grooves (millimeters):

$$k = \bar{Y}_{peak} - \bar{Y}_{groove} \qquad (9)$$

Schäffler also stated that k = 8.9 Ra. This equation establishes a relationship between the measured roughness parameter and the physical surface roughness elements that actually influence the flow.

Figure 19 shows a typical surface roughness trace and a definition of k.

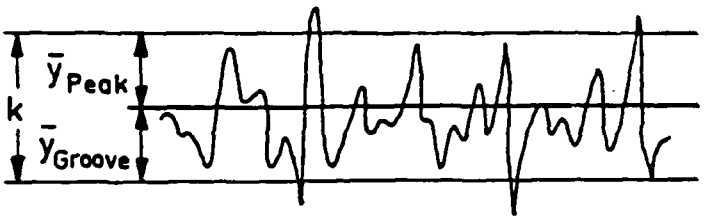

Figure 19. Roughness Parameter, k

APPENDIX B: Boundary Layer Velocity Profiles

This appendix contains plots of the composite boundary layer velocity profiles for configurations 3 thru 5.

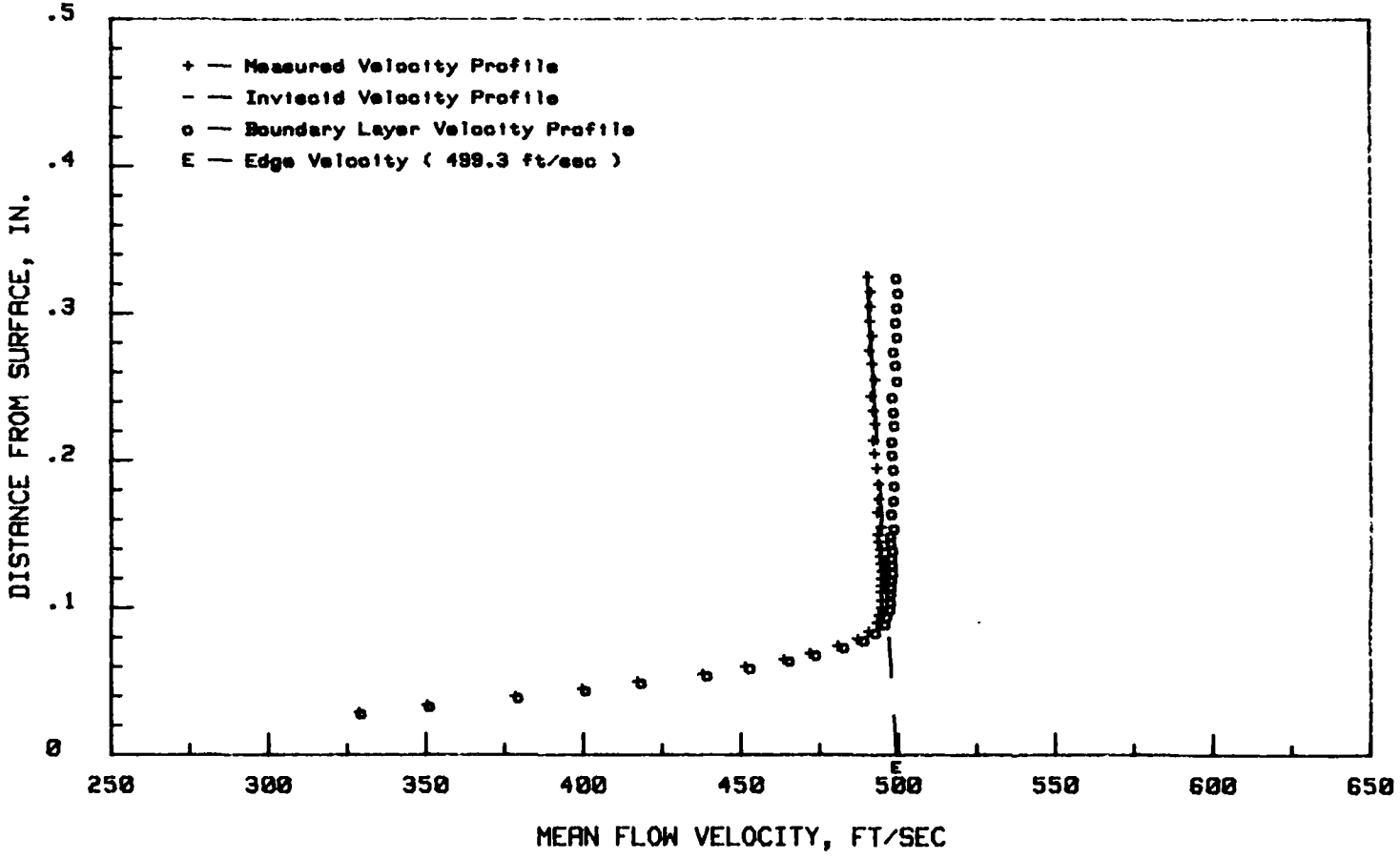

Figure 22. Boundary Layer Velocity Profile, Conf. No. 3, 86.4 Percent Chord: Ra=19.5 microns

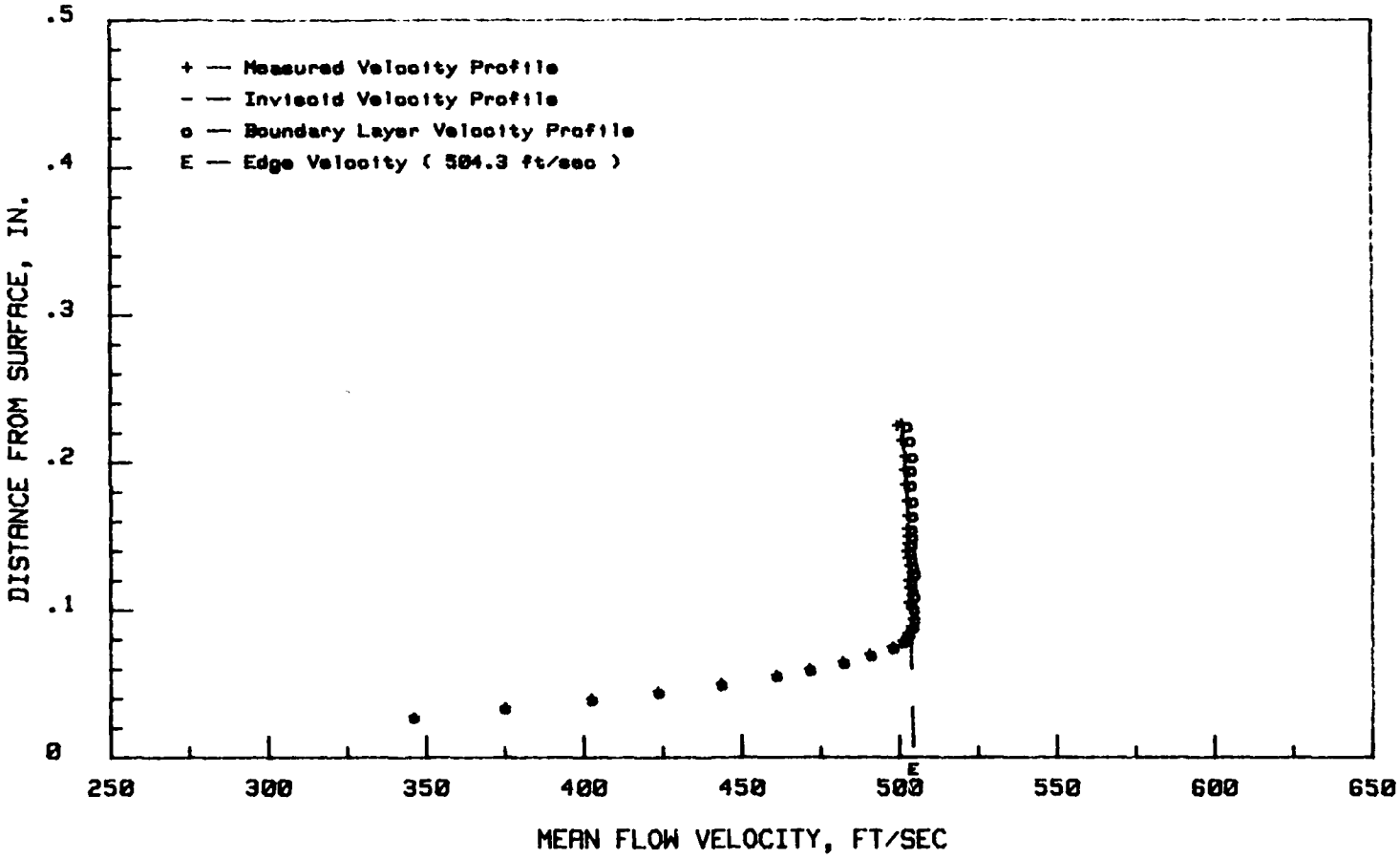

Figure 23. Boundary Layer Velocity Profile, Conf. No. 3, 78.75 Percent Chord: Ra=19.5 microns

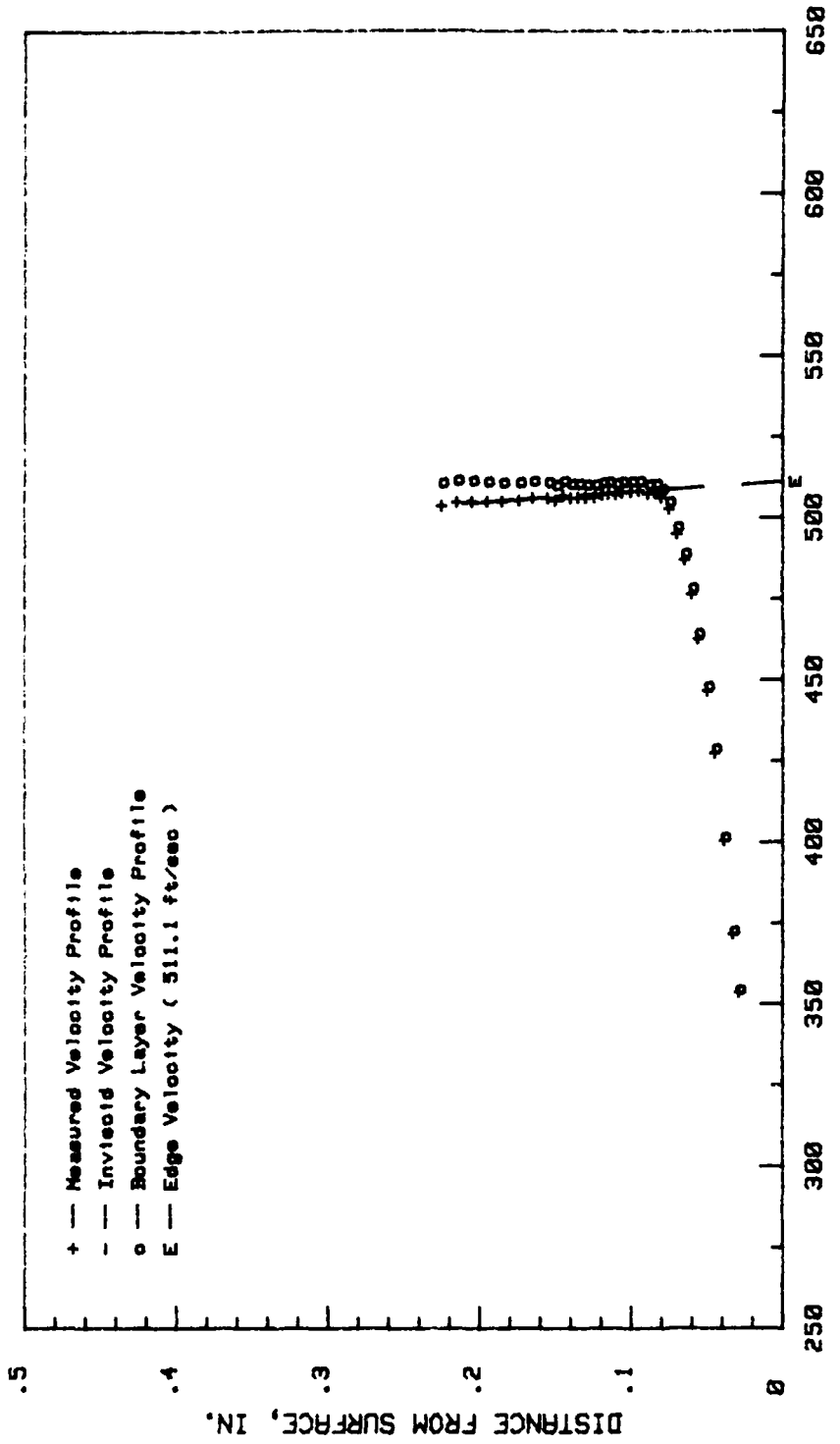

Figure 24. Boundary Layer Velocity Profile, Conf. No. 3, 74.75 Percent Chord: Ra=19.5 microns

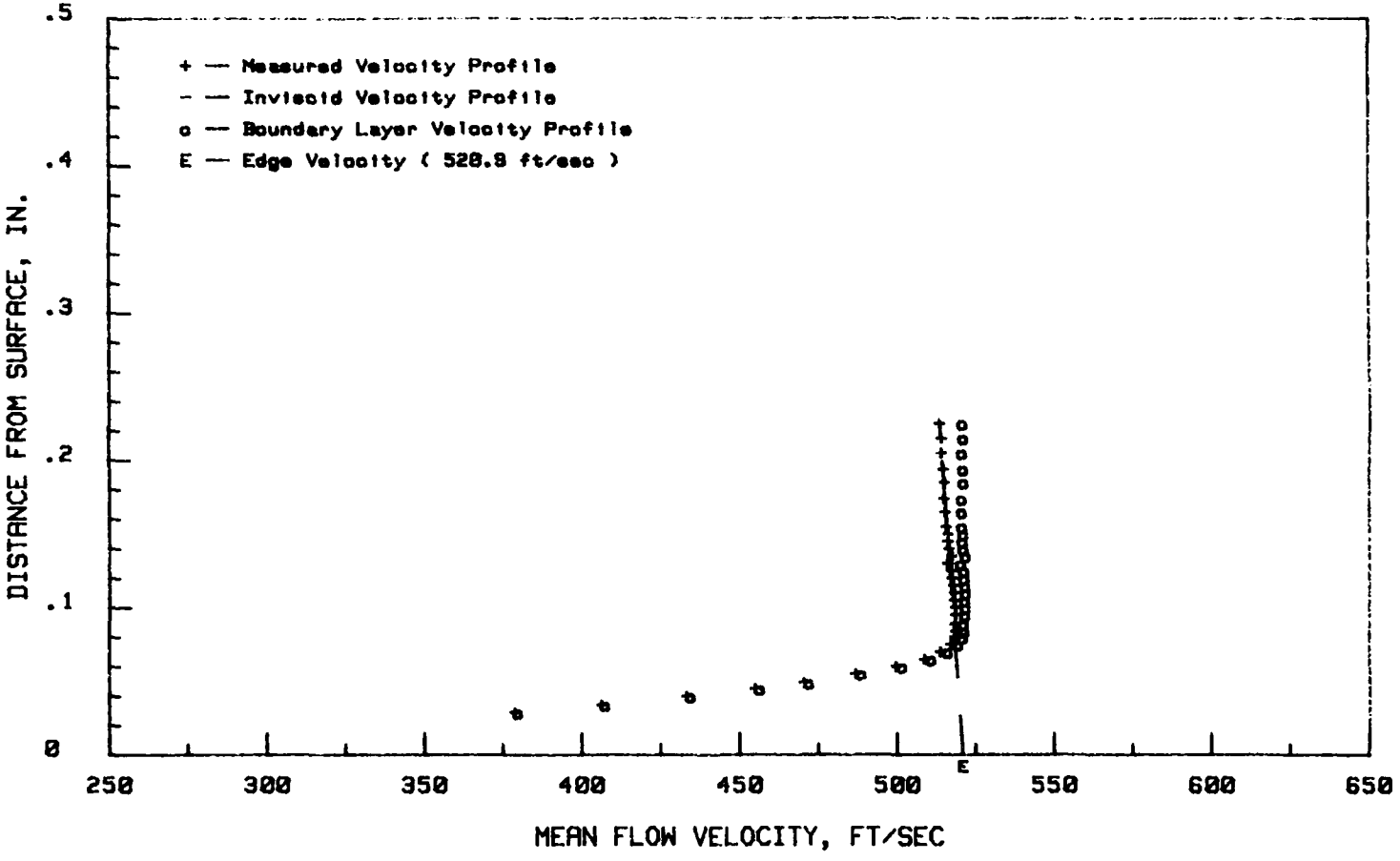

Figure 25. Boundary Layer Velocity Profile, Conf. No. 3, 66.75 Percent Chord: Ra=19.5 microns

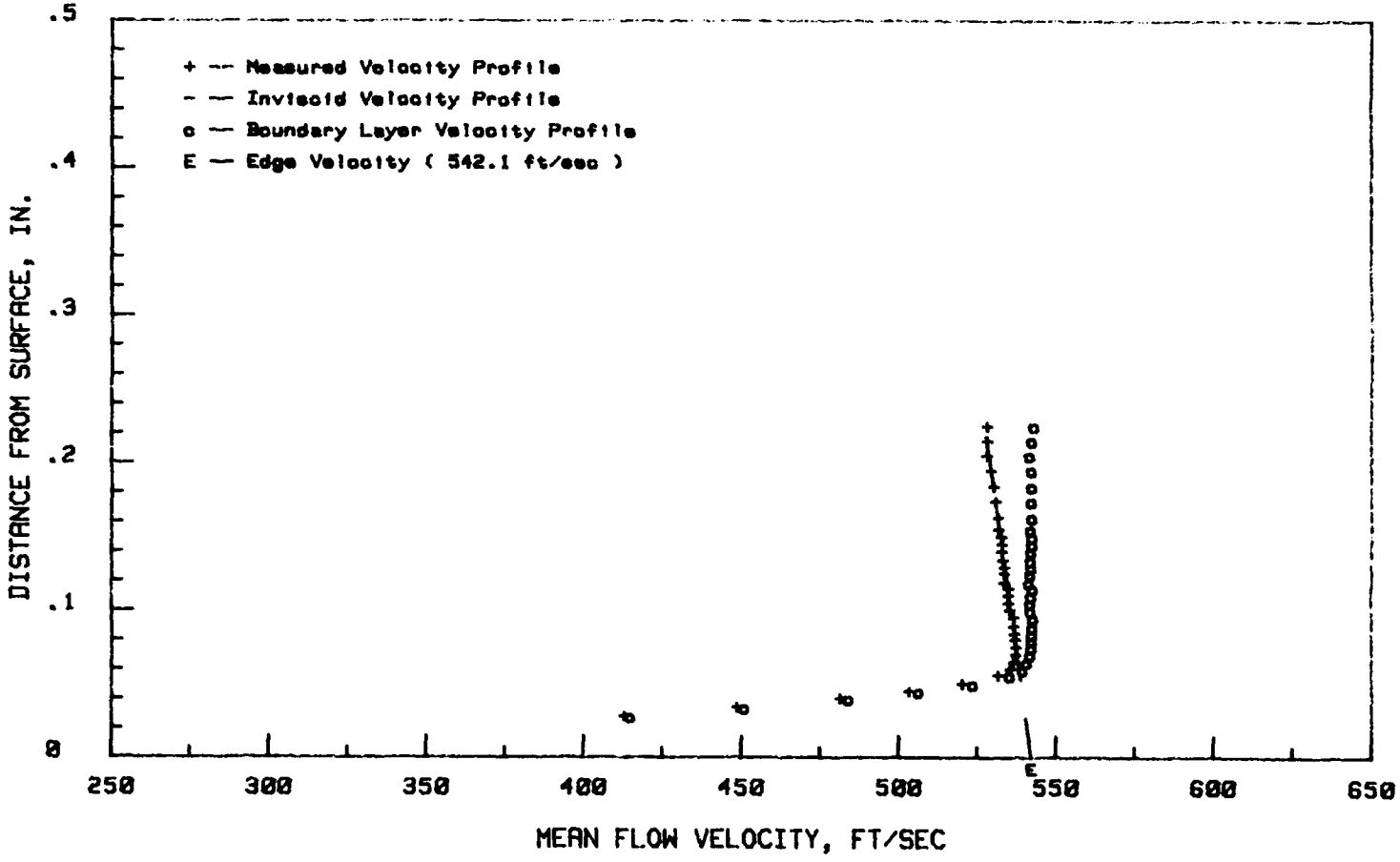

Figure 26. Boundary Layer Velocity Profile, Conf. No. 3, 50.75 Percent Chord: Ra=19.5 microns

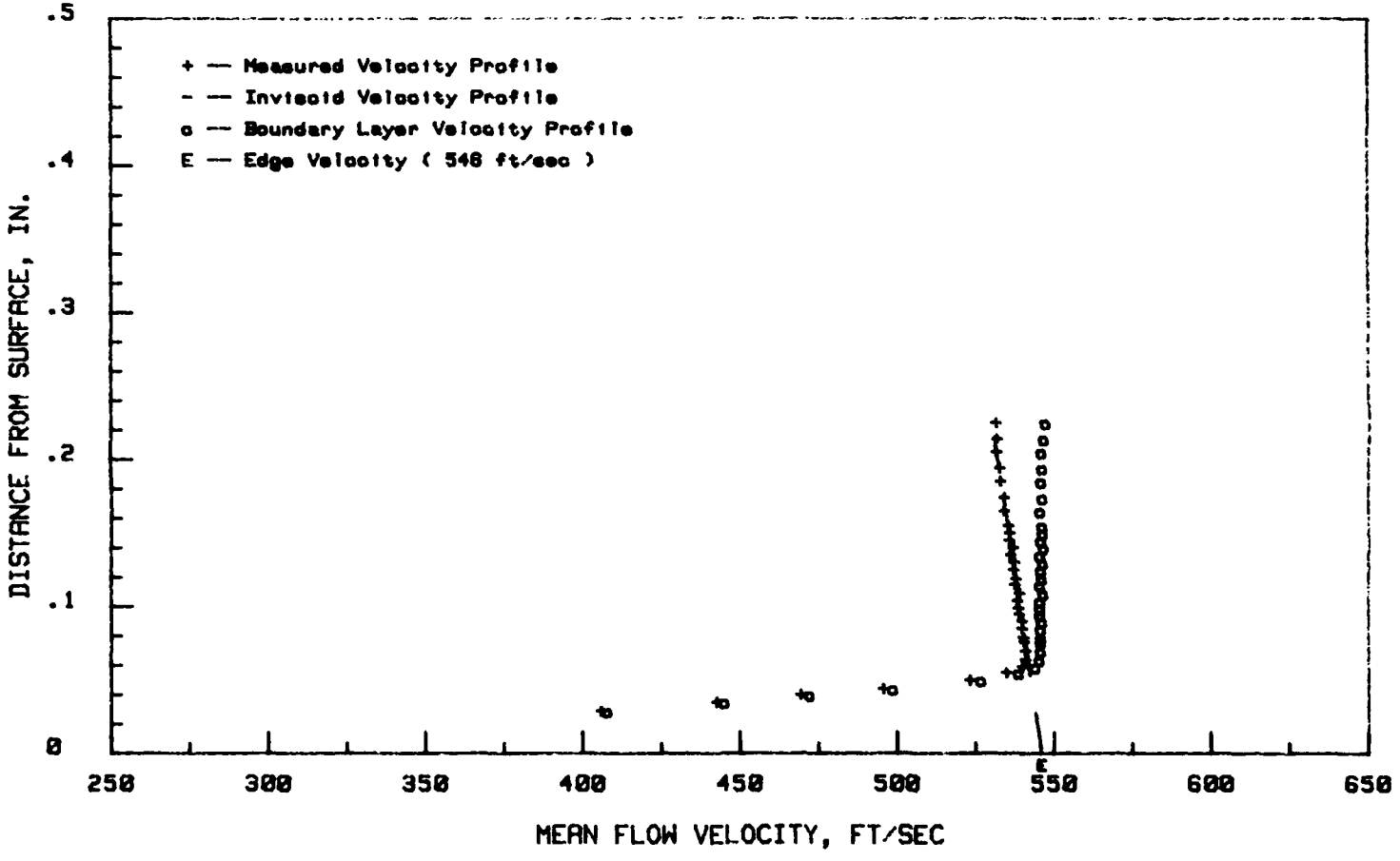

Figure 27. Boundary Layer Velocity Profile, Conf. No. 3, 42.75 Percent Chord: Ra=19.5 microns

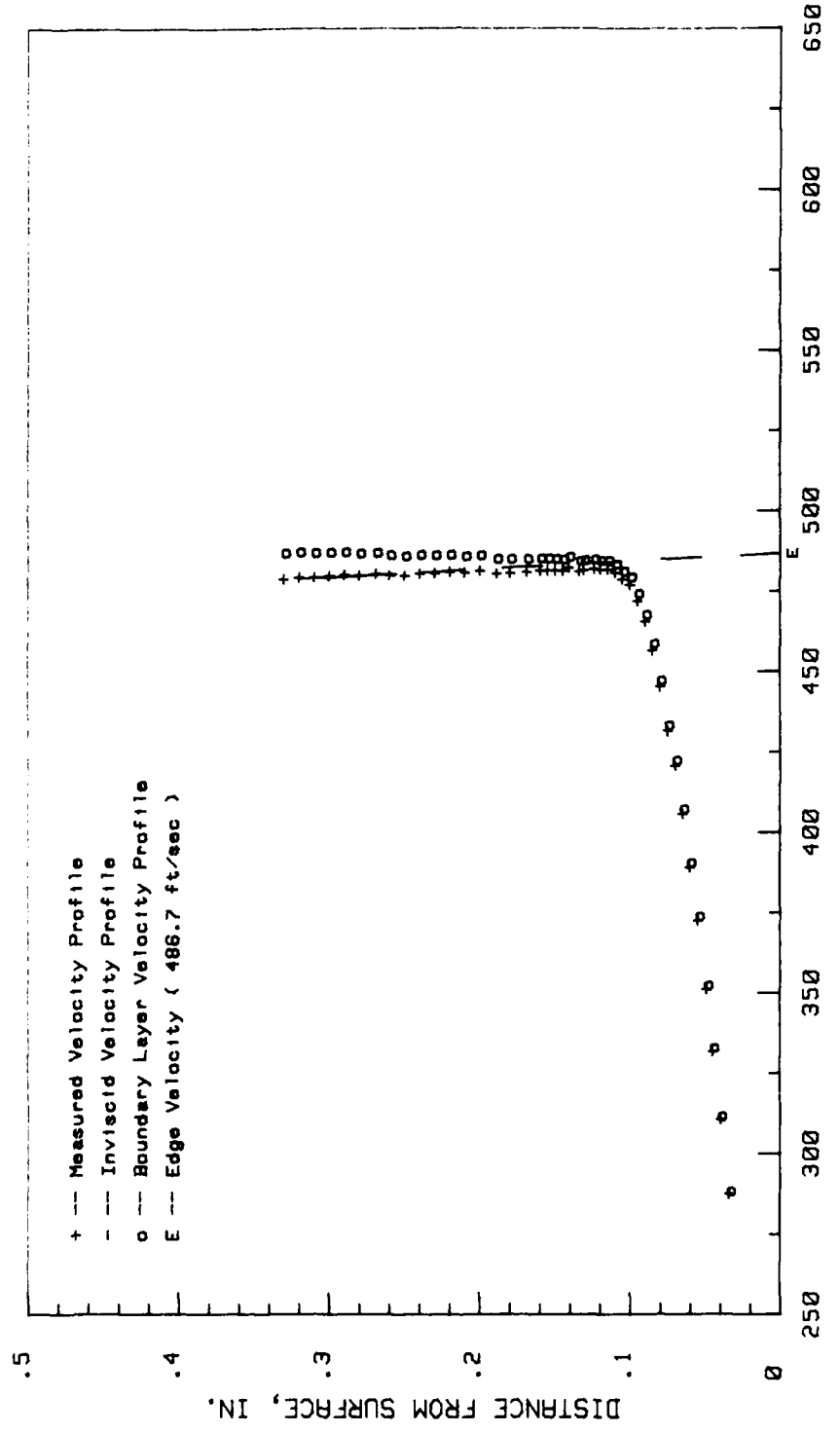

Figure 28. Boundary Layer Velocity Profile, Conf. No. 4, 86.4 Percent Chord: Ra=24.8 microns

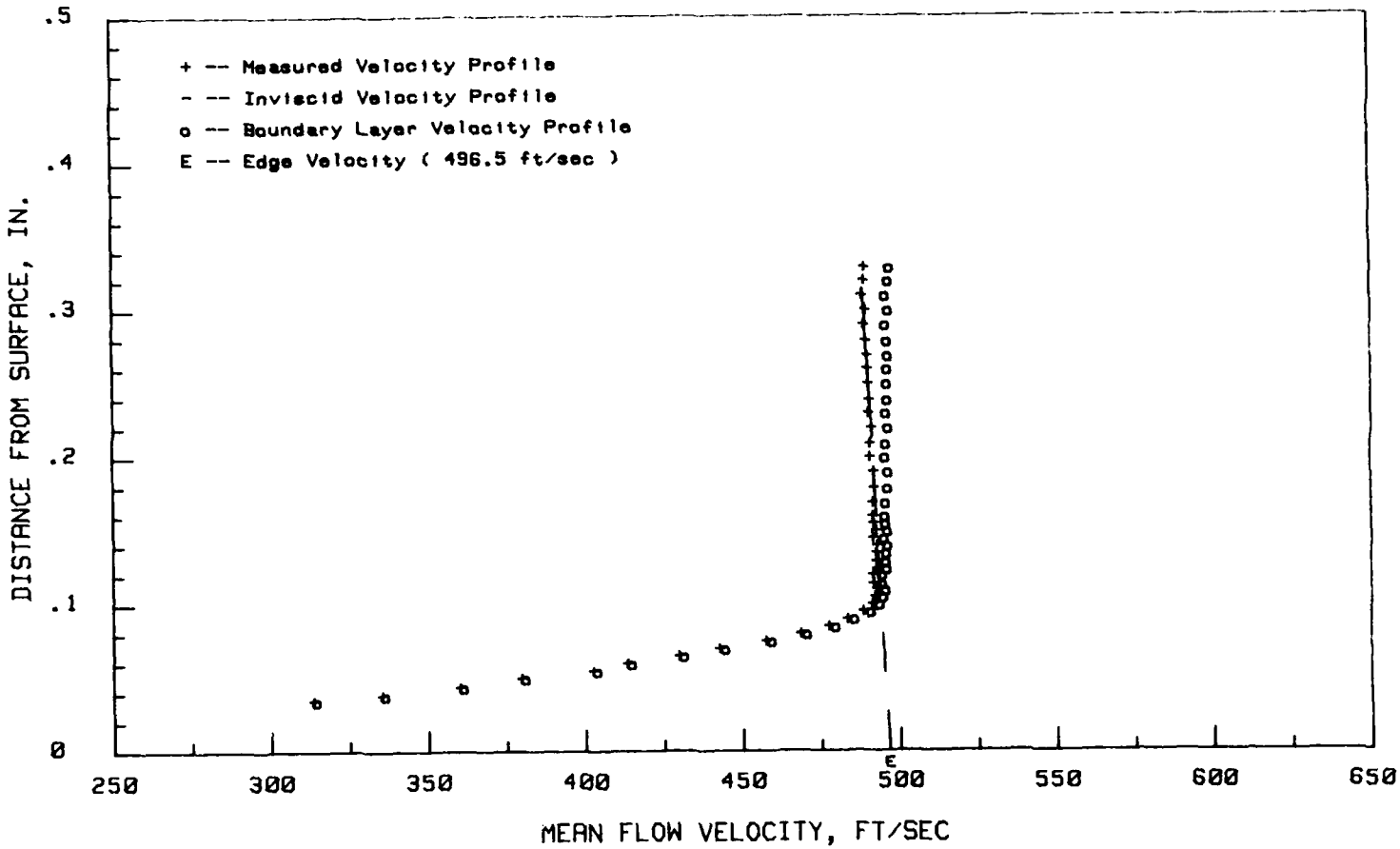

Figure 29. Boundary Layer Velocity Profile, Conf. No. 4, 78.75 Percent Chord: Ra=24.8 microns

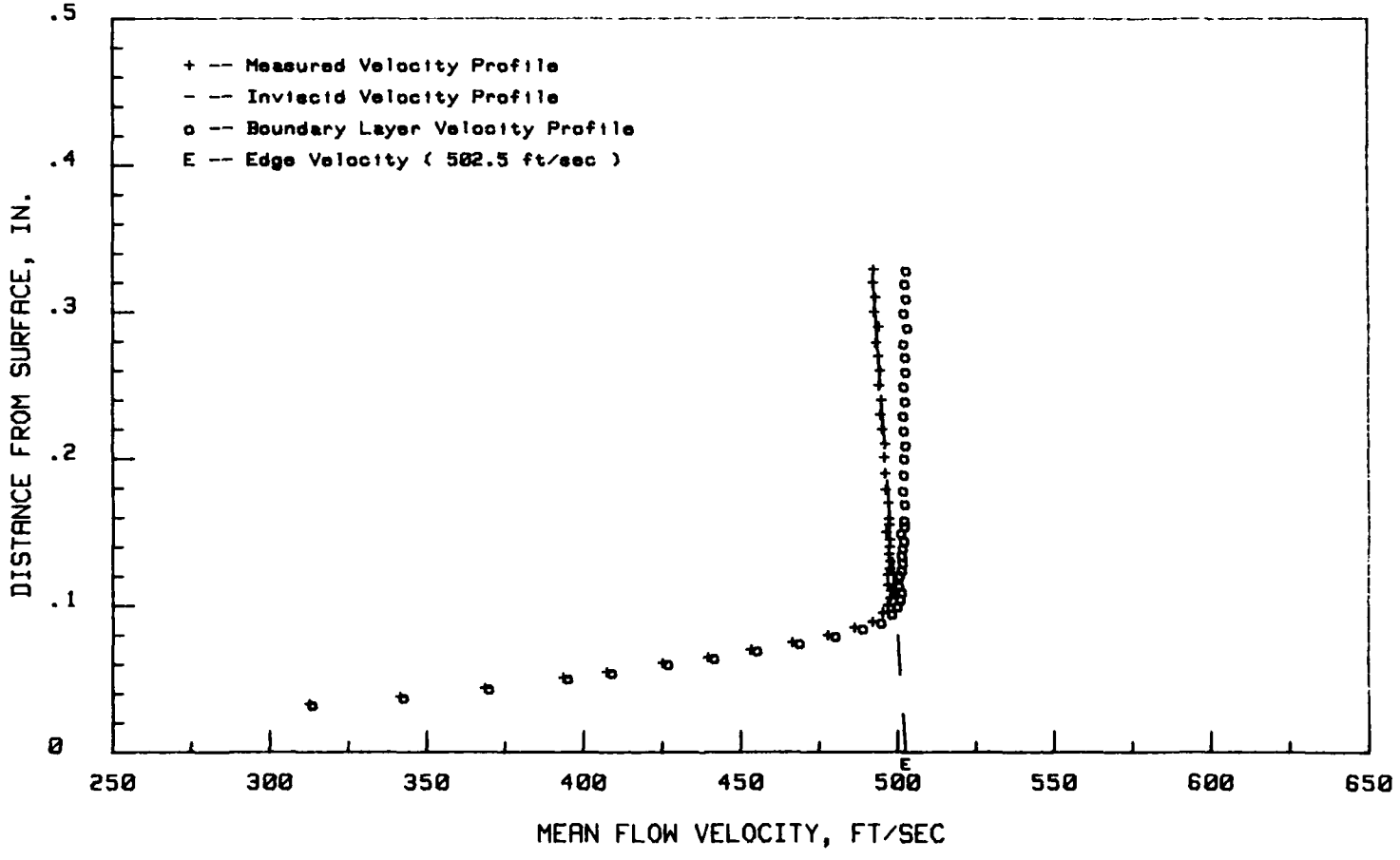

Figure 30. Boundary Layer Velocity Profile, Conf. No. 4, 74.75 Percent Chord: Ra=24.8 microns

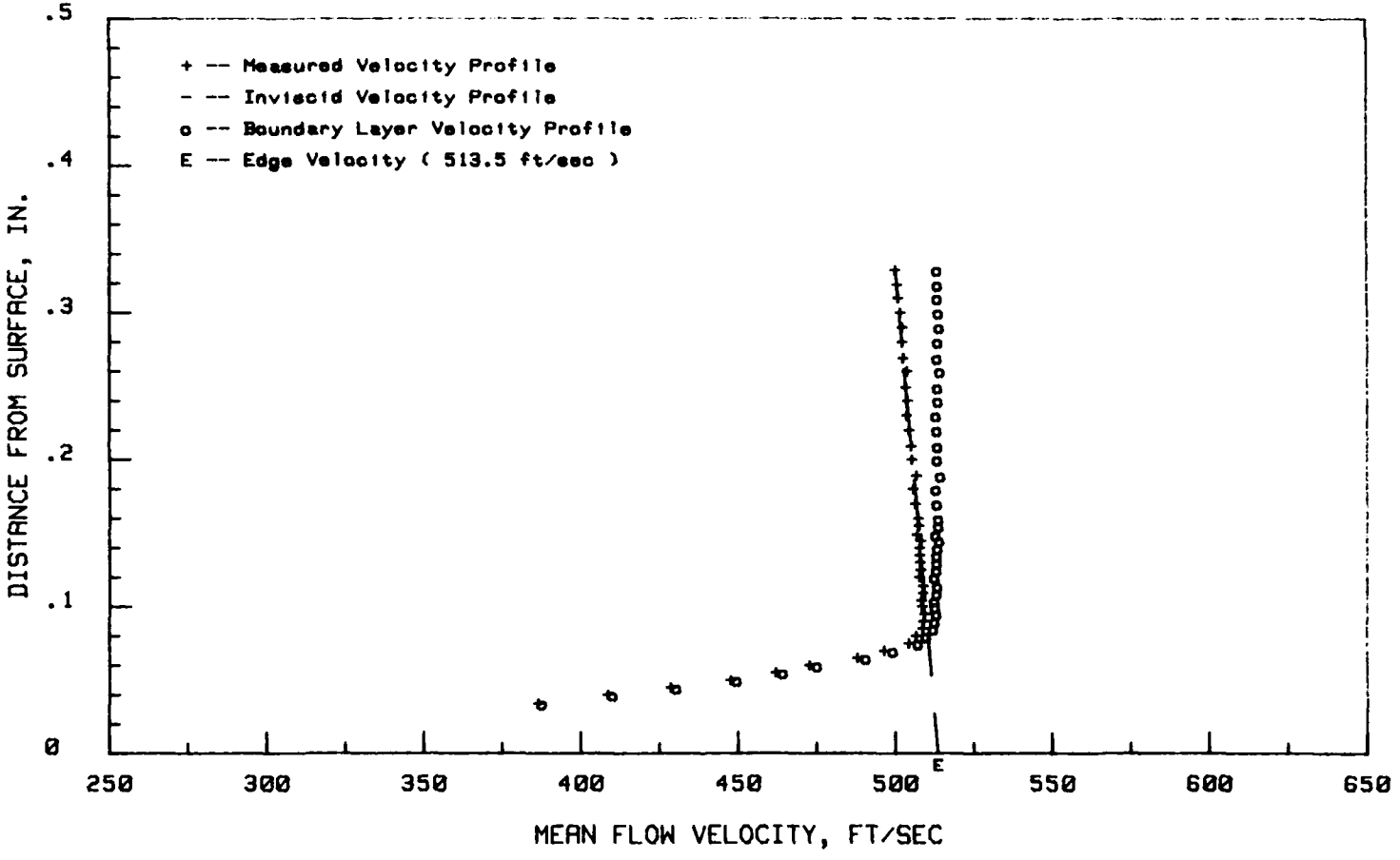

Figure 31. Boundary Layer Velocity Profile, Conf. No. 4, 66.75 Percent Chord: Ra=24.8 microns

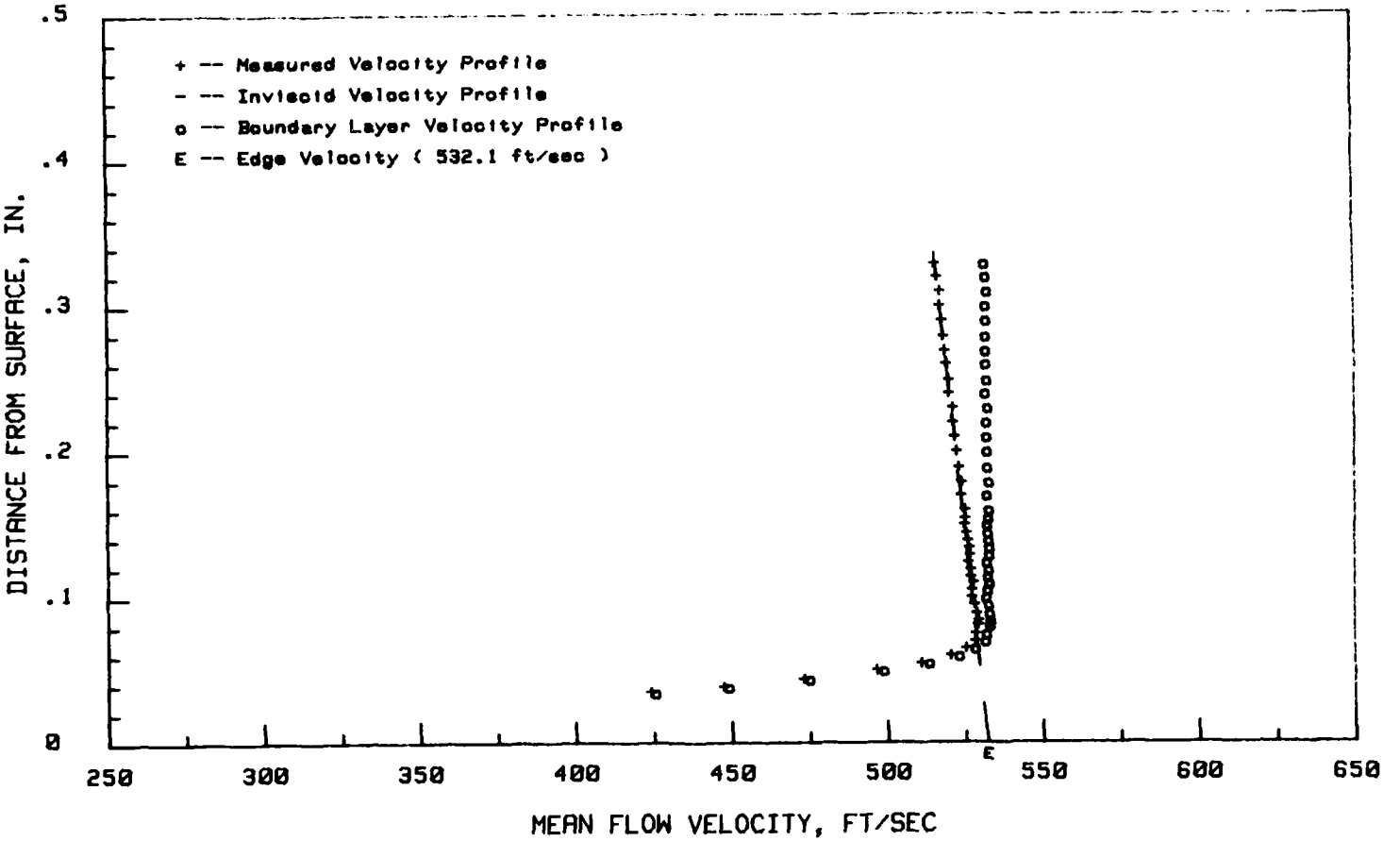

Figure 32. Boundary Layer Velocity Profile, Conf. No. 4, 50.75 Percent Chord: Ra=24.8 microns

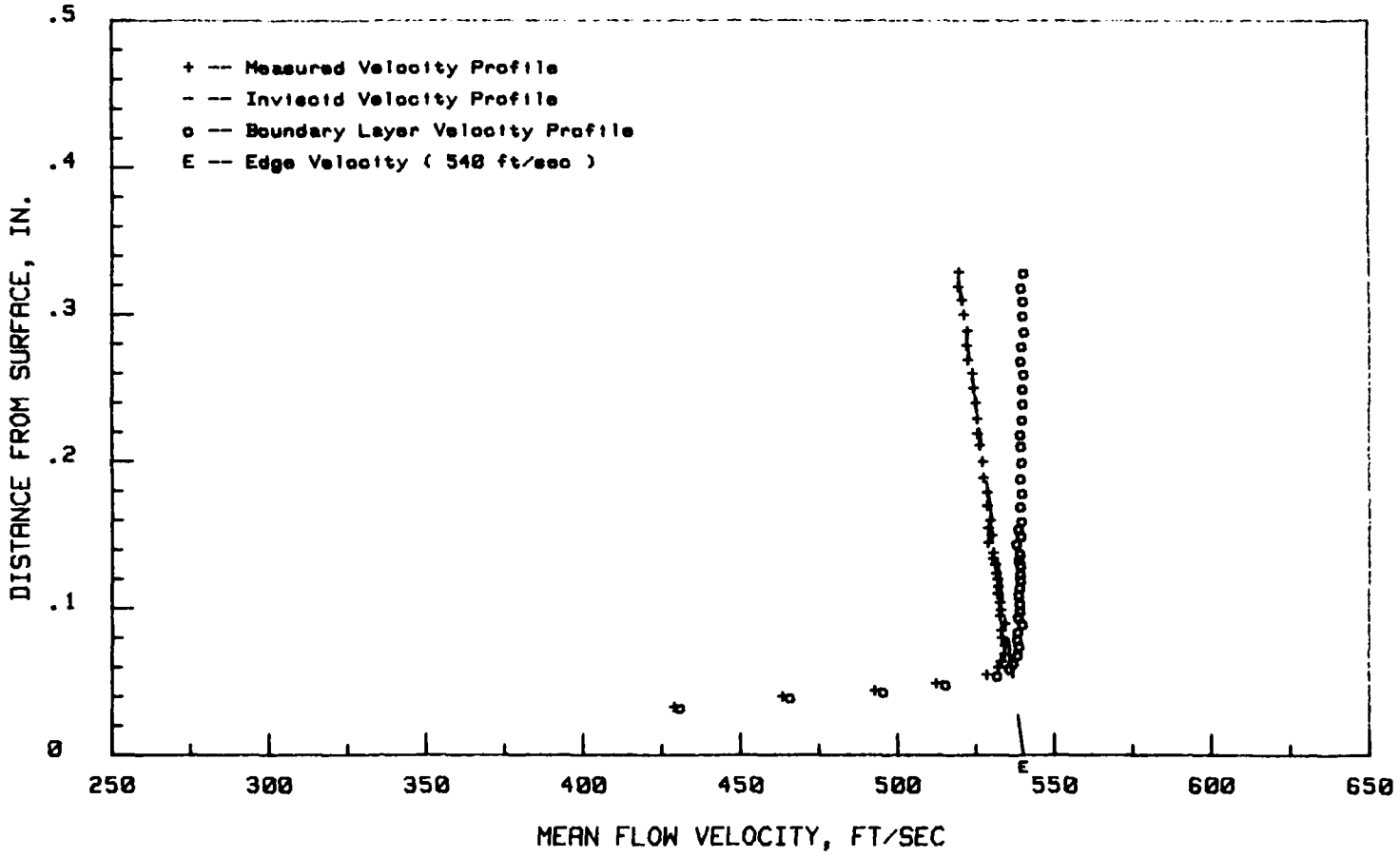

Figure 33. Boundary Layer Velocity Profile, Conf. No. 4, 42.75 Percent Chord: Ra=24.8 microns

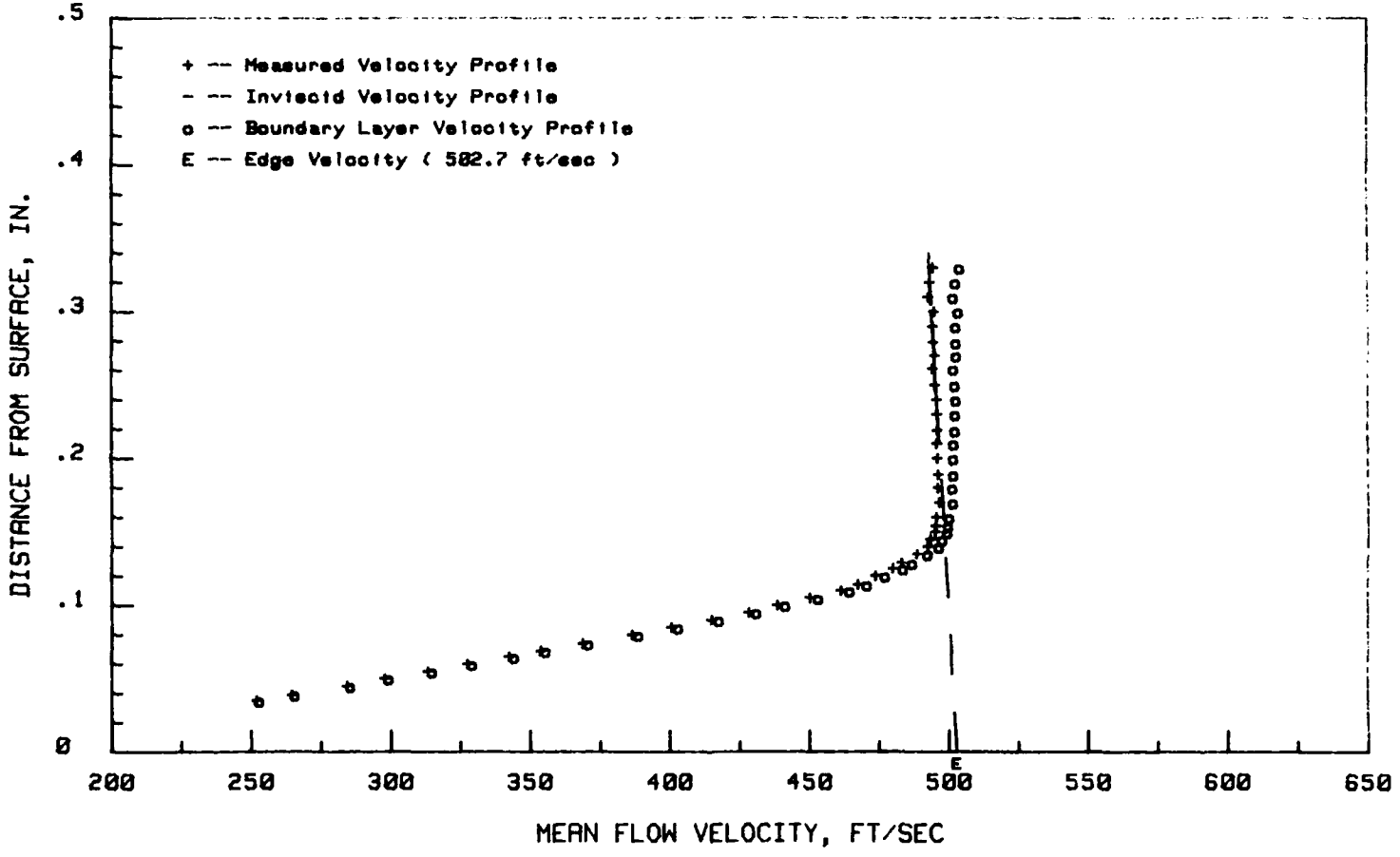

Figure 34. Boundary Layer Velocity Profile, Conf. No. 5, 86.4 Percent Chord: Ra=53.8 microns

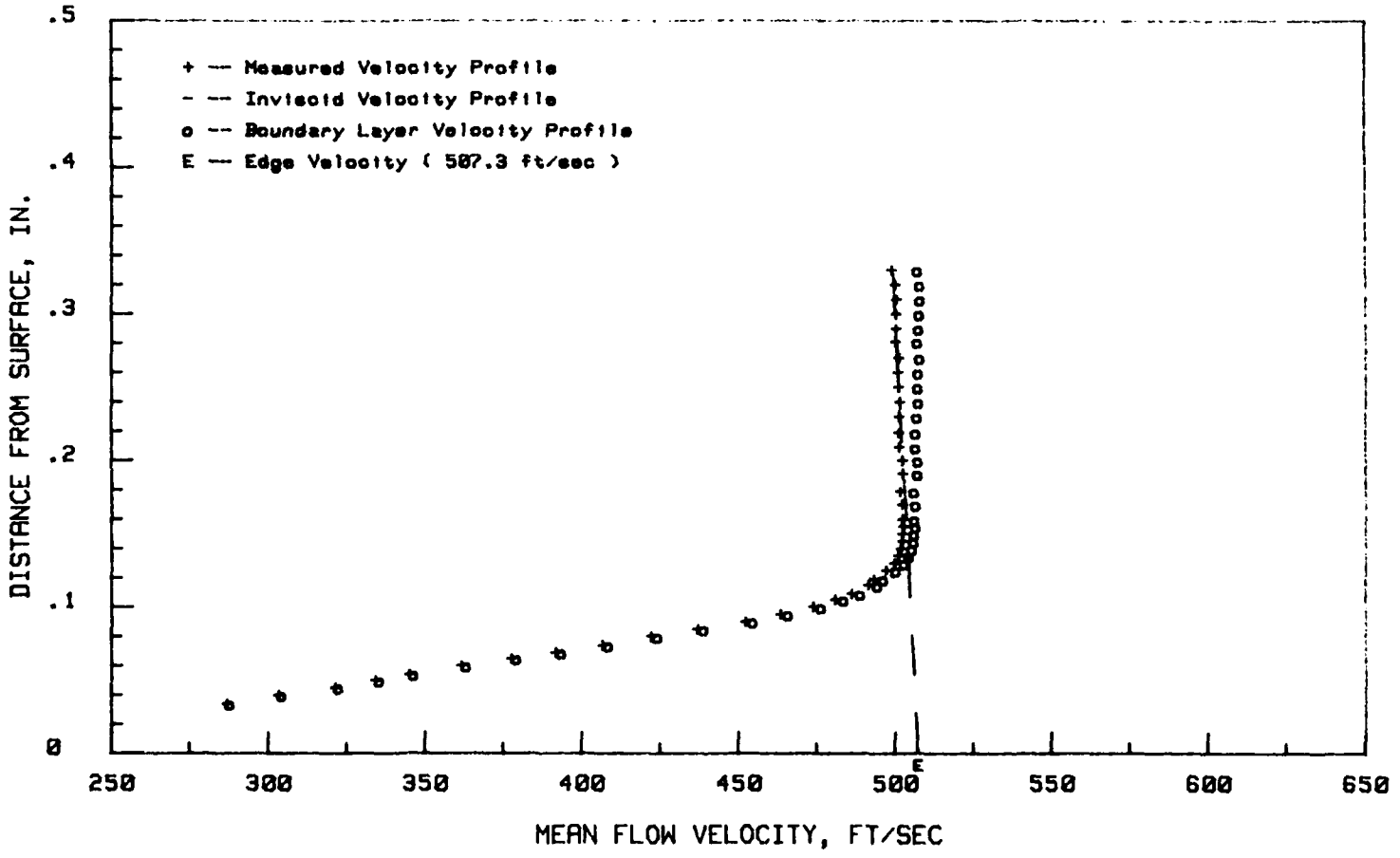

Figure 35. Boundary Layer Velocity Profile, Conf. No. 5, 78.75 Percent Chord: Ra=53.8 microns

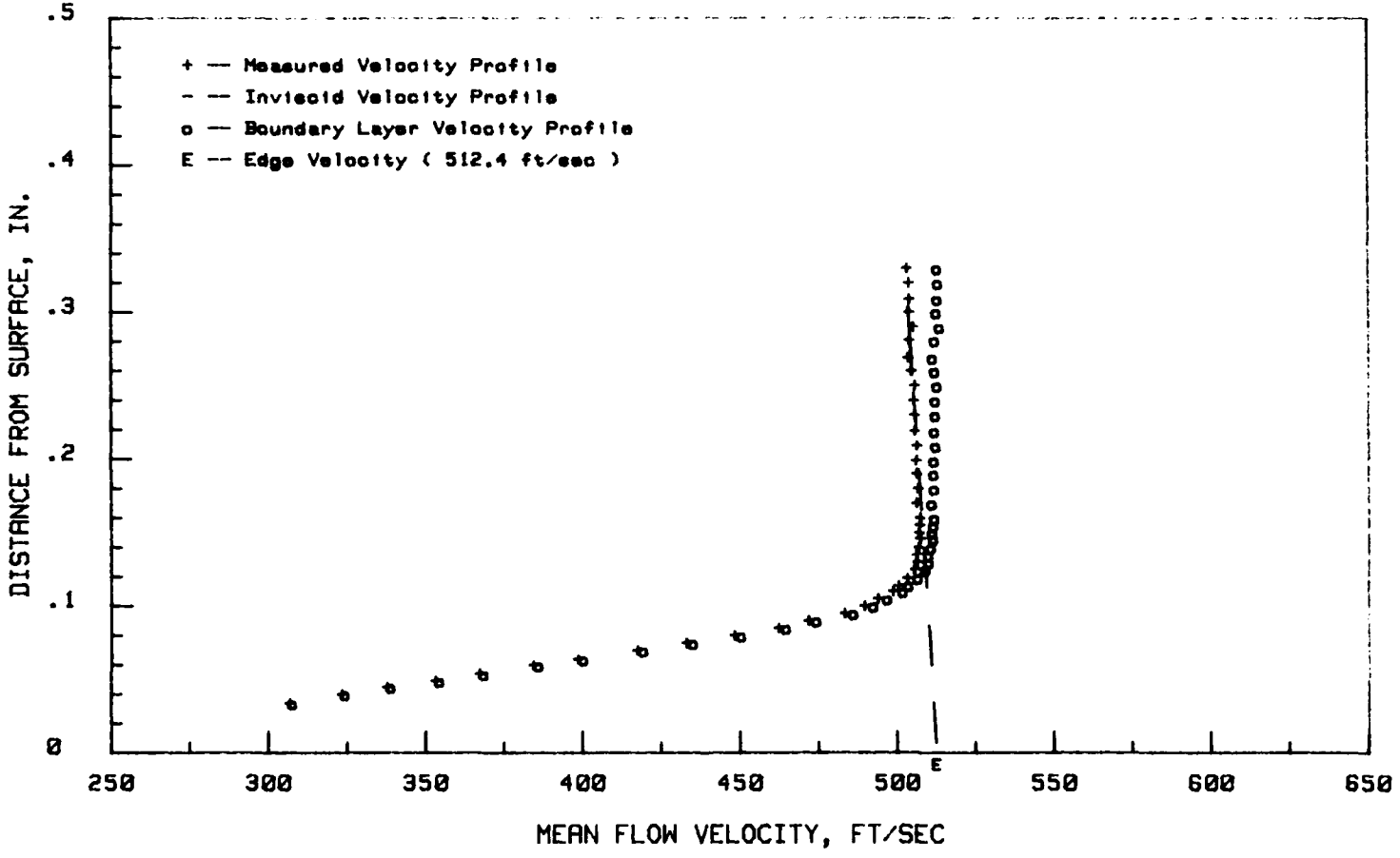

Figure 36. Boundary Layer Velocity Profile, Conf. No. 5, 74.75 Percent Chord: Ra=53.8 microns

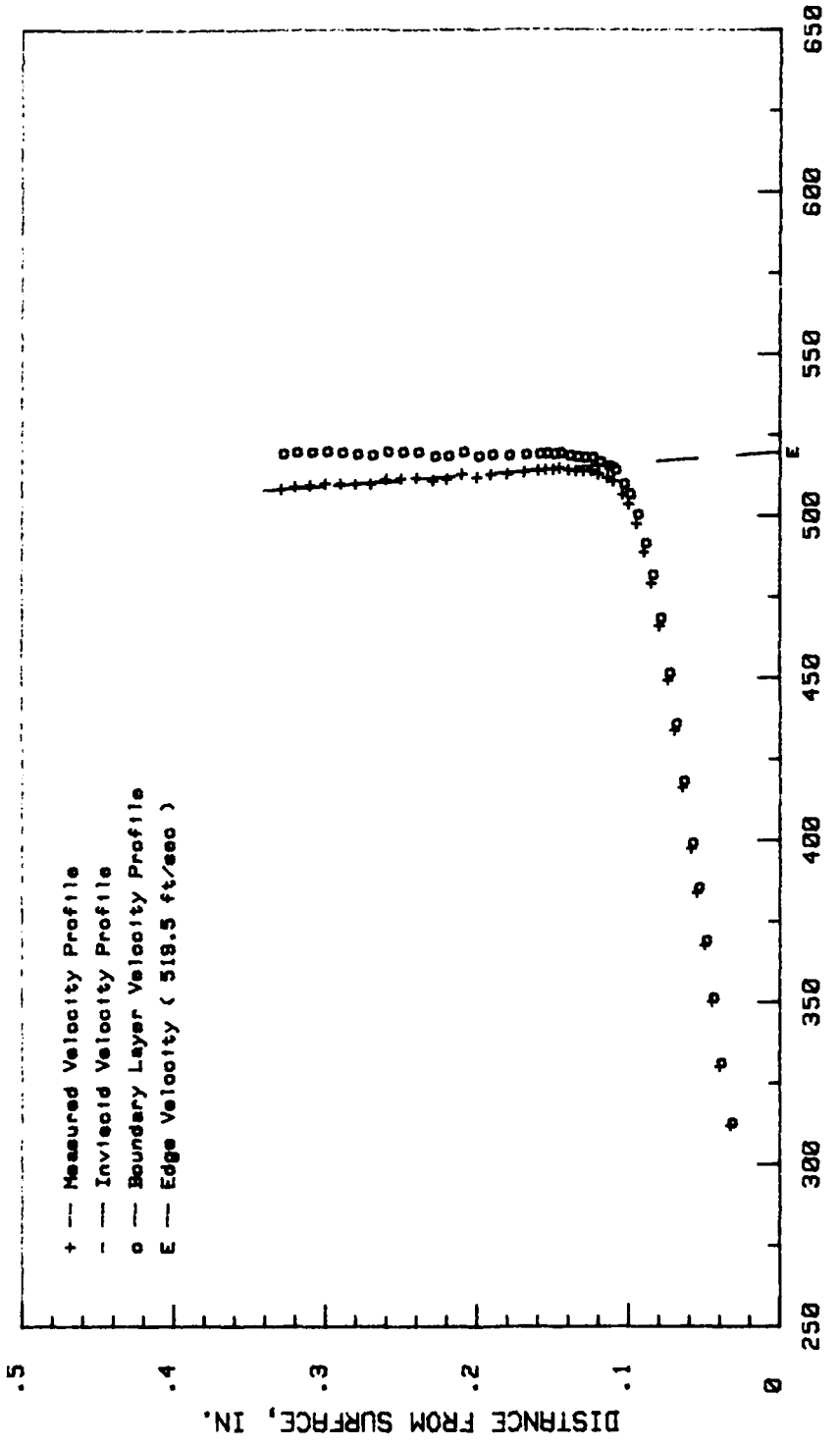

Figure 37. Boundary Layer Velocity Profile, Conf. No. 5, 66.75 Percent Chord: Re=53.8 microns

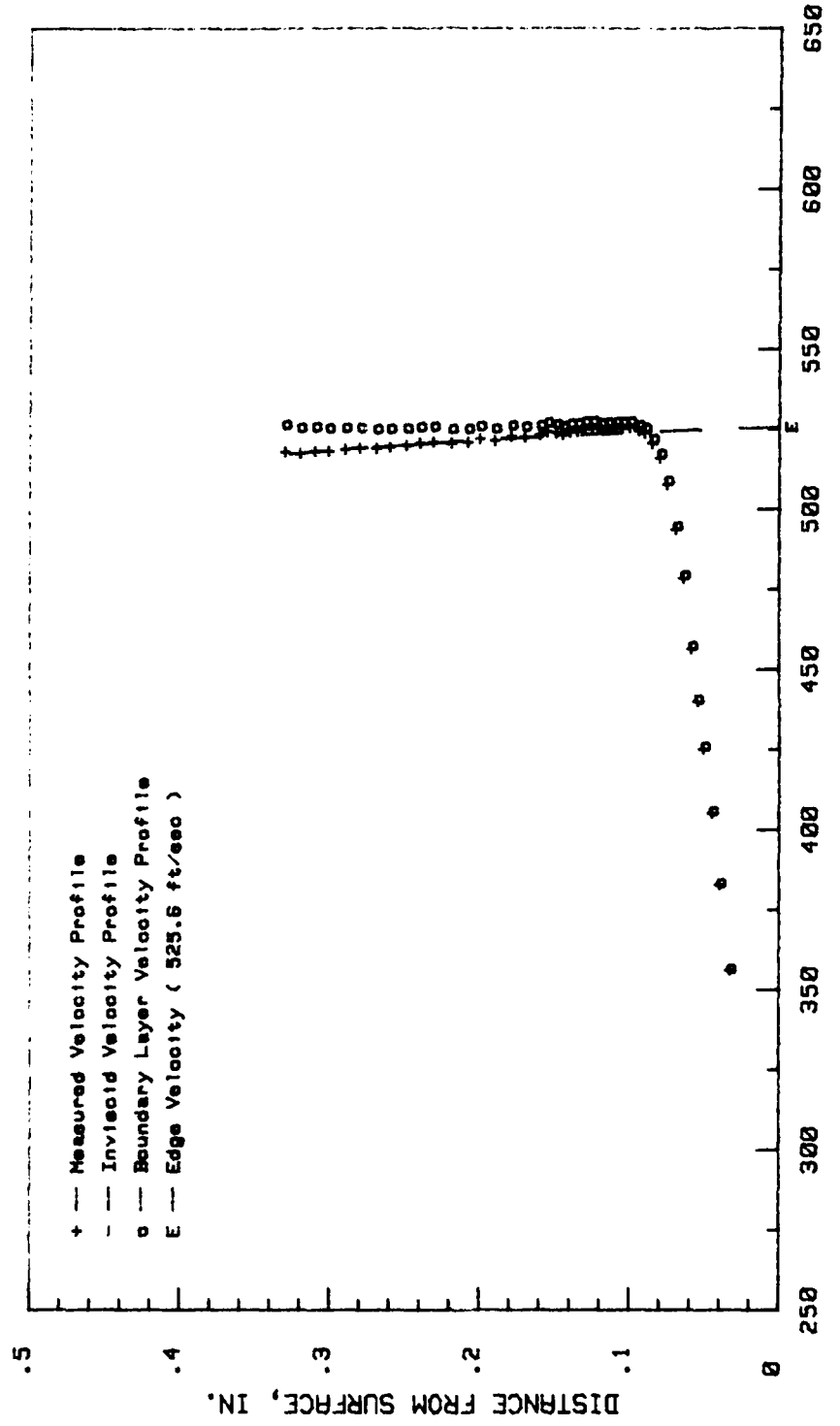

Figure 38. Boundary Layer Velocity Profile, Conf. No. 5, 50.75 Percent Chord: Ra=53.8 microns

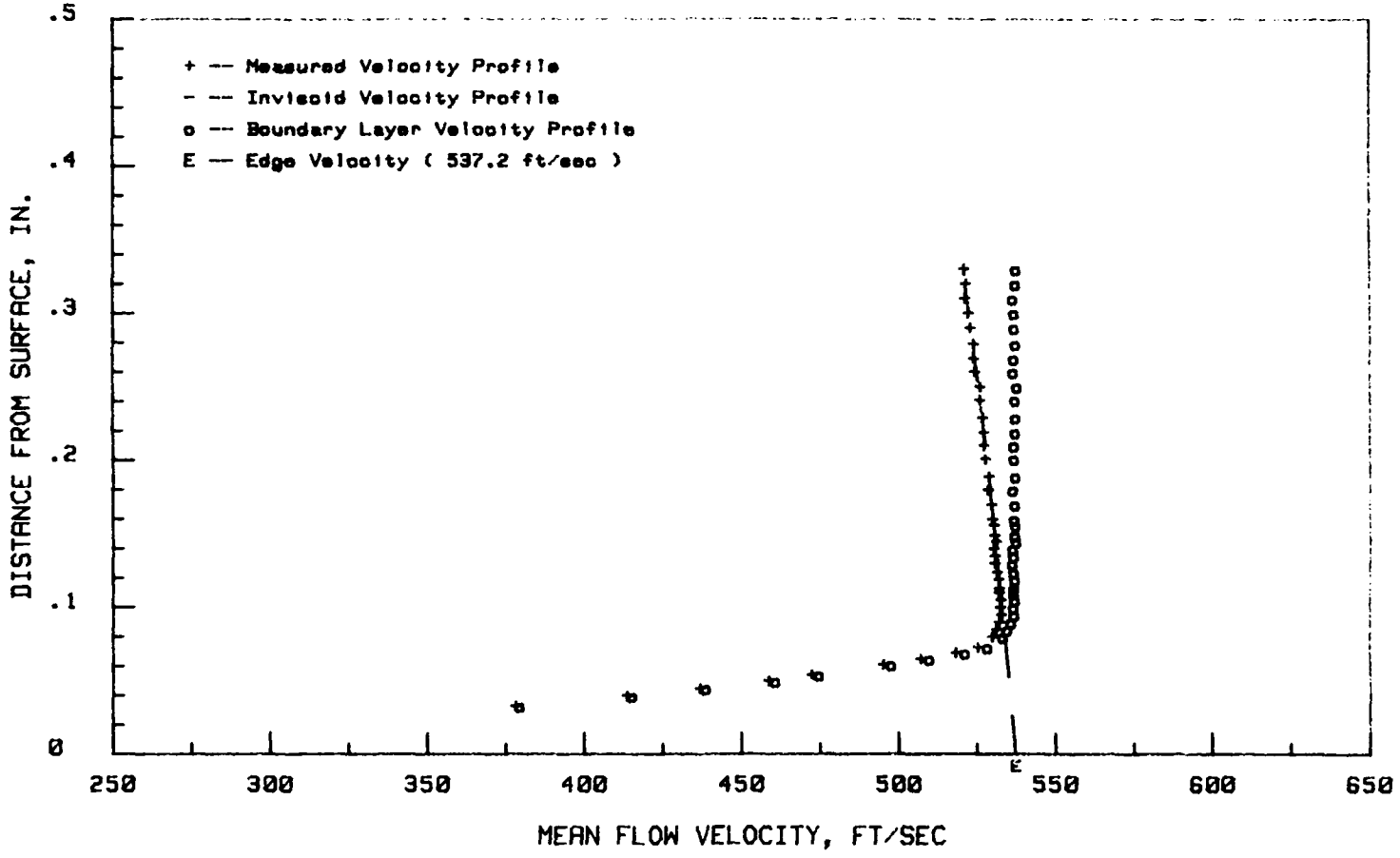

Figure 39. Boundary Layer Velocity Profile, Conf. No. 5, 42.75 Percent Chord: Ra=53.8 microns

Bibliography

1. Allison, Dennis M. Design and Evaluation of a Cascade Test Facility, MS Thesis GAE/AA/81D-2. School of Engineering, Air Force Institute of Technology (AU), Wright-Patterson AFB OH, December 1981.

2. Bammert, K. and Woelk, G. "The Influence of the Blading Surface Roughness on the Aerodynamic Behavior and Characteristic of an Axial Compressor," Journal of Engineering for Power, 102: 283-287 (April 1980).

3. Bammert, K. and Sandstede, H. "Influence of Manufacturing Tolerances and Surface Roughness of Blades on the Performace of turbines," Journal of Engineering for Power, 29-36 (January 1976).

4. Briggs, William R. Effect of Mach Number on the Flow and Application of Compressible Effects in a Two-Dimensional Subsonic-Transonic Compressor Cascade Having Varied Porous-Wall Suction at the Blade Tips, Technical Note No. 2649, National Advisory Committee on Aeronautics.

5. Cebeci, T., Mosinskis, G., and Smith, A. "Calculation of Separation Points in Incompressible Turbulent Flows," Journal of Aircraft, 9: 618-624 (September 1972).

6. Deutsch, A. and Zierke, N. The Boundary Layer on Compressor Cascade Blades, NASA-CR-173514: Semiannual Progress Report, 1 December 1983 - 1 June 1984.

7. Erwin, John R. and Emery, James C. "Effect of Tunnel Configuration and Testing Technique on Cascade Performance," Report No. 1016, National Advisory Committee on Aeronautics, 263-277, 1951.

8. Gerald, Curtis. Applied Numerical Analysis, Second Edition, Reading: Addison-Wesley, 1978.

9. Kock, C. and Smith, L. "Loss Sources and Magnitudes in Axial Flow Compressors," Journal of Engineering for Power, 411-424 (July 1976).

10. Moe, Gary P. Influence of Surface Roughness on Compressor Blades at High Reynolds Number in a Two-Dimensional Cascade, MS Thesis GAE/AA/84D-19. School of Engineering, Air Force Institute of Technology (AU), Wright-Patterson AFB OH, December 1984.

11. Oka, S. and Kostic, F. "Influence of Wall Proximity on Hot-Wire Velocity Measurements," DISA Information 13: 29-33 (May 1972).

12. Saxena, V., Shrivastava, K., and Agrawal, P., "Effect of Surface Roughness over the Blade in Compressor Cascade," Journal of the Institute of Engineers (India), 61: 54-58 (September 1980).

13. Schäffler, A. "Experimental and Analytical Investigation of the Effects of Reynolds Number and Blade Surface Roughness on Multistage Axial Flow Compressors," Journal of Engineering for Power, 102: 5-13 (January 1980).

14. Schlichting, Hermann. Boundary Layer Theory, Seventh Edition, New York; McGraw-Hill, 1979.

15. Tanis, Frederick J. Roughness Effect on Compressor Blade Performance in Cascade at High Reynolds Number, MS Thesis GAE/AA/83D-23. School of Engineering, Air Force Institute of Technology (AU), Wright-Patterson AFB OH, December 1983.

VITA

Captain Larry D. Williams was born on 26 October 1952 in Clarksville, Texas. He graduated from Clarksville High School in 1971. He attended Jarvis Christian College from 1971 until he entered the U. S. Air Force in 1973. He was accepted into the Airman Education and Commissioning Program in 1976 and attended the University of Texas at Arlington. He graduated in 1980 with the degree of Bachelor of Science in Aerospace Engineering. Following graduation, he attended Officer Training School, Medina AFB, Texas. He was assigned in September 1980 to the Deputy for Engineering, Flight Systems Engineering, Aeronautical Systems Division, Wright-Patterson AFB as an Aircraft Propulsion Performance engineer until entering the School of Engineering, Air Force Institute of Technology, in May 1984. He is a member of Tau Beta Pi.

Permanent address: 702 South Falls
Clarksville, Texas 75426

UNCLASSIFIED
SECURITY CLASSIFICATION OF THIS PAGE

AD-A163974

REPORT DOCUMENTATION PAGE

1a. REPORT SECURITY CLASSIFICATION UNCLASSIFIED	1b. RESTRICTIVE MARKINGS
2a. SECURITY CLASSIFICATION AUTHORITY	3. DISTRIBUTION/AVAILABILITY OF REPORT Approved for public release; distribution unlimited.
2b. DECLASSIFICATION/DOWNGRADING SCHEDULE	
4. PERFORMING ORGANIZATION REPORT NUMBER(S) AFIT/GAE/AA/85D-17	5. MONITORING ORGANIZATION REPORT NUMBER(S)
6a. NAME OF PERFORMING ORGANIZATION School of Engineering 6b. OFFICE SYMBOL (If applicable) AFIT/ENY	7a. NAME OF MONITORING ORGANIZATION
6c. ADDRESS (City, State and ZIP Code) Air Force Institute of Technology Wright-Patterson AFB, OH 45433	7b. ADDRESS (City, State and ZIP Code)
8a. NAME OF FUNDING/SPONSORING ORGANIZATION 8b. OFFICE SYMBOL (If applicable)	9. PROCUREMENT INSTRUMENT IDENTIFICATION NUMBER
8c. ADDRESS (City, State and ZIP Code)	10. SOURCE OF FUNDING NOS. PROGRAM ELEMENT NO. / PROJECT NO. / TASK NO. / WORK UNIT NO.
11. TITLE (Include Security Classification) See Box 19	
12. PERSONAL AUTHOR(S) Williams, Larry Donal, B.S., Capt. USAF	
13a. TYPE OF REPORT MS Thesis 13b. TIME COVERED FROM _____ TO _____	14. DATE OF REPORT (Yr., Mo., Day) 1985 December 15. PAGE COUNT 84
16. SUPPLEMENTARY NOTATION	

17. COSATI CODES		
FIELD	GROUP	SUB. GR.
21	05	

18. SUBJECT TERMS (Continue on reverse if necessary and identify by block number)
Cascade Testing, Pressure Distribution, Roughness Effects, Compressor Blades, Boundary Layer

19. ABSTRACT (Continue on reverse if necessary and identify by block number)

Thesis Title: EFFECTS OF SURFACE ROUGHNESS ON PRESSURE DISTRIBUTION AND BOUNDARY LAYER OVER COMPRESSOR BLADES AT HIGH REYNOLDS NUMBER IN A TWO-DIMENSIONAL CASCADE

Advisor: Dr. William C. Elrod

Approved for public release: IAW AFR 190-1.
LYNN E. WOLAVER 16 JAN 86
Dean for Research and Professional Development
Air Force Institute of Technology (AFC)
Wright-Patterson AFB OH 45433

20. DISTRIBUTION/AVAILABILITY OF ABSTRACT UNCLASSIFIED/UNLIMITED ☒ SAME AS RPT. ☐ DTIC USERS ☐	21. ABSTRACT SECURITY CLASSIFICATION UNCLASSIFIED
22a. NAME OF RESPONSIBLE INDIVIDUAL William C. Elrod	22b TELEPHONE NUMBER (Include Area Code) 513-255-3517 22c OFFICE SYMBOL AFIT/ENY

DD FORM 1473, 83 APR EDITION OF 1 JAN 73 IS OBSOLETE.

UNCLASSIFIED
SECURITY CLASSIFICATION OF THIS PAGE

An evaluation of the effects of surface roughness on the pressure distribution and boundary layer over compressor blades in a two-dimensional cascade has been completed. The cascade consisted of seven NACA 65-A506 airfoils with a two inch chord and an aspect ratio of one. The blades were set in the test section at an angle of attack of 15 degrees. The test section unit Reynolds number for the evaluation was in excess of two million per foot.

The changes to the cascade blade pressure distribution were minimal for moderate average roughness (Ra=24.8 microns) to low average roughness values (Ra=.18 micron), except for pressures near the leading edge which were more pronounced. The pressure distribution for a blade surface roughness of 53.8 microns differed considerably from the baseline case.

The cascade test blade experienced laminar separation with turbulent reattachment at moderate to low roughness levels, and fully turbulent flow at high roughness levels. The blade suction surface boundary layer thickness increased with roughness values but was most responsive to the transition from laminar to turbulent flow.

END

FILMED

3-86

DTIC